Stony Brook University

A Study of the Extratropical Tropopause: Related to the Upper Tropospheric Relative Vorticity and the Distance from the Jet

A Thesis Presented

by

Shu Meir Wang

to

The Graduate School

in Partial fulfillment of the

Requirements

for the Degree of

Master of Science

in

Marine and Atmospheric Science

Stony Brook University

December 2011

Stony Brook University

The Graduate School

Shu Meir Wang

We, the thesis committee for the above candidate for the

Master of Science degree, hereby recommend

acceptance of this thesis.

Professor Marvin A. Geller

School of Marine and Atmospheric Science

Professor Brian A. Colle

School of Marine and Atmospheric Science

Professor Sultan Hameed

School of Marine and Atmospheric Science

This thesis is accepted by the Graduate School

Lawrence Martin

Dean of the Graduate School

Abstract of the Thesis

A Study of the Extratropical Tropopause: Related to the Upper Tropospheric Relative Vorticity and the Distance from the Jet

By

Shu Meir Wang

Master of Science

in

Marine and Atmospheric Science

Stony Brook University

2011

The extratropical tropopause is a familiar feature in meteorology; however, the understanding of the mechanisms for its existence, formation, maintenance and sharpness is still an active area of research. In order to examine the sharpness of the tropopause, Birner et al. (2002) proposed the concept of the TIL (Tropopause Inversion Layer), which is based upon the characteristics of the thermal profile. Bell and Geller (2008), believing that the resulting stability profile was more fundamental to dynamics and transport, defined the ESTL (Extratropical Stability Transition Layer) based on the stability characteristics.

Wirth (2004) suggested that the cyclonic/anticyclonic asymmetry plays a large role in the sharpening of the climatological TIL. Son and Polvani (2007) also showed that TIL sharpness was greater when the upper troposphere relative vorticity was anticyclonic than when there was cyclonic relative vorticity in their simplified atmospheric general circulation models. In contrast to this picture, we are finding that the location of the point where the extratropical tropopause is being determined with respect to the jet might be a more important factor in determining the height of extratropical tropopause. Furthermore, since Bell and Geller (2008) showed that the depth of the ESTL is mainly determined by the height of the extratropical tropopause, the same would be true of the sharpness. This may at first seem like a semantic argument, but we believe that there is an important distinction of the physical processes involved if the upper tropospheric vorticity is the dominant mechanism compared with the situation when the location with respect to the jet is dominant.

In this study, three stations in the United States are used to examine the association between the tropopause height and the distance from the jet, and by comparison of the correlations between the tropopause height and the distance from the

jet and that between the tropopause height and the upper tropospheric relative vorticity, the one which is more important in determining the tropopause height can be seen. We found that the distance from the jet is a more important in determining the tropopause height for the two northern stations, and for the south most station, the two correlations are statistically similar.

Table of Contents

List of Figures

List of Tables

List of Abbreviations

AWC: Aviation Weather Center
CONUS: Continental United States
CPT: Cold Point Tropopause
EMC: Environmental Modeling Center
ESTL: Extratropical Stability Transition Layer
GEMPAK: general meteorology package
GUIs: Graphical User Interfaces
GR: Global Reanalysis
HPS: Hydrologic Prediction Center
IGRA: Integrated Global Radiosonde Archive
LRT: Lapse Rate Tropopause
MPC: Marine Prediction Center
NARR: North American Regional Reanalysis
NASA: National Aeronautics and Space Administration
NCDC: National Climate Data Center
NCEP: National Centers for Environmental Prediction
NSF: National Science Foundation
OFCM: Office of the Federal Coordinator for Meteorology
ppmv: parts per million by volume
PV: Potential Vorticity
PVU: Potential Vorticity Unit
RDAS: Regional Data Assimilation System
RRS: Radiosonde Replacement System
SPARC: Stratospheric Processes and their Role in Climate
SPC: Storm Prediction Center
TIL: Tropopause Inversion Layer
TPC: Tropical Prediction Center
WBAN: Weather-Bureau-Army-Navy
WMO: World Meteorological Organization

1. Introduction

The extratropical tropopause is the transition layer between the turbulent troposphere, which is the lowest layer of the atmosphere where temperature decreases with height at an average lapse rate around 6.5°C km^{-1}, and the stably stratified stratosphere, which is the layer above the troposphere where the temperature does not change much with height in its lowest few kilometers and then increases with height. People have been observing the troposphere over human history since it is where all weather phenomena occur. The constituent contents of the troposphere and stratosphere are very different as well. In the troposphere, for instance, water vapor concentrations can be very high (parts per 100), whereas in the stratosphere, water vapor concentrations are only a few parts per million by volume (ppmv). On the other hand, ozone concentrations in the stratosphere are much higher than in unpolluted regions in the troposphere. Vertical heat transport in the troposphere is principally by convection and baroclinic mixing, whereas radiative heat transport is dominant in the stratosphere. Therefore, understanding the physical processes that form and maintain the tropopause is important both for dynamical and chemical interactions between the troposphere and the stratosphere. In particular, the study of the mechanisms for the existence, formation, maintenance, and sharpness of the extratropical tropopause is an active area of research. In this work, I try to explore one small facet of this problem, which contributes to this area of research.

1.1 Definition of the Tropopause

The easiest way to define the tropopause height is to use the thermal definition officially accepted by the World Meteorological Organization (WMO 1957); that is to say, the lowest level at which the environmental lapse rate (-dT/dz) becomes less than 2K/km for at least 2 kilometers. Some other definitions such as the "cold point tropopause" (Highwood and Hoskins 1998) or the "top of the convective cloud layer" (Manabe and Strickler 1964) can also be useful, especially in the tropics. An alternative method to locate the tropopause height is to use the dynamics-based definition, where the critical value of 2 PVU (potential vorticity units, where 1 PVU is 10^{-6} kg^{-1} m^2s^{-1}) is often used to define the extratropical tropopause height (Hoerling et al. 1991). This value is chosen because it approximates the thermal tropopause, and also has a better dynamic foundation (Hoskins et al. 1985). In the tropics, the distance between the thermal tropopause and cold-point tropopause can be on the order of kilometers; however, the varying definitions of tropopause height converge to similar values in the extratropical region.

1.2 The Physical Mechanisms Maintaining Extratropical Tropopause

Stone (1978) proposed the theory of Baroclinic Adjustment, which suggests that the critical shear for baroclinic instability can be related to the meridional temperature gradient and concludes that baroclinic eddy fluxes are responsible for maintaining the tropospheric lapse rate near its critical value in the extratropics. Held (1982) tried to pair up the dynamical constraints, using Charney's baroclinic instability model, with the radiative constraint of radiative equilibrium in the stratosphere to determine the tropopause altitude distribution. Lindzen (1993) developed a similar treatment, where he

took the extratropical troposphere to achieve a baroclinically neutral state using the Eady model for baroclinic instability. A minimum meridional wavenumber is established by the width of the subtropical jet, and neutrality is established by moving the tropopause to a sufficient height so that the total wavenumber corresponds to the short-wave cutoff in the Eady (1949) problem. Lindzen (1993) found the resulting height to be close to the observed tropopause height. Thuburn and Craig (1997) performed general circulation model experiments where they altered parameters such as the boundary temperature, the boundary temperature gradient, and the planet's rotation rate to show that Lindzen's (1993) arguments did not predict the relationship between the fluid depth scale height and the modeled tropopause height. By these means, Thuburn and Craig (1997) concluded that baroclinic adjustment is not the only mechanism constraining the tropopause height. Barry et al. (2000) tried to explain this discrepancy and concluded that the time-scales of the various baroclinic adjustments theories are the same magnitude as the radiative time-scales, so that baroclinic adjustment is too slow to bring the atmosphere into a baroclinically neutral state.

Haynes et al. (2001) used an idealized general circulation model to show that sharp extratropical tropopause can be obtained purely by the dynamical mixing effect of baroclinic eddies against a thermally relaxed equilibrium state, in a statistical equilibrium sense.

1.3 The Sharpness of the Extratropical Tropopause

Recently, the works of Birner et al. (2002) and Birner (2006) have motivated much research activity. Birner et al. (2002) presented climatological calculations for two stations in Germany based on a high vertical-resolution radiosonde data set for a ten-year period (1990-1999). He showed fine-scale structure evident at the tropopause using the WMO thermal tropopause as the geophysical reference level, which was quite different from the structure presented in standard climatologies (see figure 1.1). Birner (2006) expanded this work on the extratropical tropopause region to the US operated upper air stations in North America and showed that the fine-scale structure evident in the German climatologies were not a local phenomenon. Also, he showed that the winds and vertical shear exhibited fine-scale structure at the tropopause consistent with thermal wind balance. The tropopause-based climatologies for four west coast United States stations (see figure 1.2) showed that the tropopause is characterized by a much sharper temperature profile with a temperature inversion just above the tropopause level. This corresponded to an increasing buoyancy frequency (static stability) below the tropopause and a very sharp gradient in the static stability just above the tropopause which then decays approximately exponentially back to typical stratospheric stability values. He describes the increasing temperature with height just above the tropopause as the tropopause inversion layer (TIL), which is based upon the characteristics of thermal profile. Bell and Geller (2008), believing that the resulting stability profile was more fundamental to dynamics and transport, defined the ESTL (Extratropical Stability Transition Layer), which is the depth from the maximum value of stability (the overshoot value) right above the tropopause to the local minimum value of stability in the stratosphere, based on the stability characteristics (see figure 1.3). Bell and Geller (2008) showed that this inversion layer exists in all seasons for both tropical and extratropical regions, with clear seasonal variations in depth. The global and persistent character of the

TIL has potentially significant implications for chemical transport across the extratropical tropopause, and for the dynamical coupling between the stratosphere and the troposphere.

Wirth (2003) has proposed that large-scale, balanced dynamical processes might be responsible for the TIL structure. Wirth (2004) suggested that the cyclonic/anticyclonic asymmetry plays a large role in the sharpening of the climatological TIL. This is based on the concept of potential vorticity conservation, $(\zeta+f)/h=$constant. That is, h is smaller when ζ is negative, anticyclonic, thus the tropopause is sharper (see figure 1.4). Son and Polvani (2007) have shown that the TIL sharpness was greater when the upper troposphere relative vorticity was anticyclonic than when there was cyclonic relative vorticity in their simplified atmospheric general circulation model, in which the only external forcing is an equilibrium temperature structure to which the model is relaxed with a fixed time scale. Randel et al. (2007) also demonstrated the Wirth cyclonic-anticyclonic TIL asymmetry with global data using GPS observations, but they noted that this asymmetry was not enough to achieve the observed sharpness. They suggested that radiative cooling in the region above the CPT (Cold Point Tropopause) provides the extra observed sharpness.

The Randel et al. (2007) and Son and Polvani (2007)'s papers were built on Wirth's concept of balanced dynamics, which suggests that a sharper extratropical tropopause should result when the relative vorticity in the upper troposphere becomes more anticyclonic, and that a less sharp extratropical tropopause results when the relative vorticity is more cyclonic. Wirth (2001) argued that this anticyclonic sharpening should dominate and lead to the observed sharpness due to nonlinearities. We have a different hypothesis. We believe that the location of the point where the extratropical tropopause is being determined with respect to the jet axis is a more important factor in determining the height of extratropical tropopause than is the upper tropospheric relative vorticity. This may at first seem like a semantic argument, but we believe that there is an important distinction between the physical processes involved if the upper tropospheric vorticity is the dominant mechanism compared with the situation when the location with respect to the jet axis is dominant.

It is well known in synoptic meteorology that the height of the tropopause on the tropical side of the jet stream is higher, and it is lower poleward of the jet stream (figure 1.5). Clearly, the variations of the upper tropospheric relative vorticity over a location are related to variations in where this location lies with respect to the jet stream as well. If an upper-level trough (ridge), is moving over a station, this would likely lead to the station lying north (south) of the jet. Thus, there should be a large correlation between the upper tropospheric relative vorticity over a station and its location with respect to the jet. Therefore, if the distance from the jet is the controlling factor in determining the height of the tropopause, then the cyclonic/anticyclonic asymmetry, suggested by Wirth would also be seen. We believe, since Wirth's concept involves balanced dynamics, which is a reversible process, it is difficult to believe that this is the dominant dynamical process in achieving the observed sharpness of the extratropical tropopause. Furthermore, since Wirth's suggestion, which involves balanced, reversible, physics, is deficient in achieving the observed sharpness, this motivated Randel et al. (2007) to suggest that sharpening by radiative processes is crucial to account for the observed sharpness, whereas if the Wirth process is not the controlling dynamical process, appealing to the need for extra sharpening may not be necessary. We believe that baroclinic mixing is the key factor for

the sharpening and lifting of the tropopause in the extratropics. Held's (1982) and Lindzen's (1993) arguments imply that the sharpness is mainly caused by the sharpening of the vertical potential vorticity (PV) gradient by baroclinic mixing of PV. This is also consistent with the results in Haynes et al. (2001), Schneider (2004), and Son and Polvani (2007). In this work, I have improved upon Bell's work (2008) which showed that the extratropical tropopause was sharpened by a dry baroclinic event.

Figure 1.6 gives some support for our argument that it is the location north or south of the jet rather than upper tropospheric relative vorticity that is the dominant control of extratropical tropopause height, and hence the depth of the ESTL. This figure shows a plot of tropopause height versus relative vorticity at Dodge City, Kansas (37.77°N, 99.97°W), from December, 2003 to February, 2004, which is similar to Figure 3 in Randel et al. (2007). Note that all of the points above the average curve correspond to when this station is south of the jet, and the lower points to when it is north of the jet. Furthermore, it is seen that the points below (when the station is north of the jet) the best-fit curve of the average tropopause height within each vorticity bin are more scattered than those above the curve (when the station is south of the jet). It has been noted that more small-scale filamentary structure is seen in the tropopause potential temperature in winter than in summer, and also more is seen poleward than equatorward of the jet (e.g., Nielson-Gammon, 2001). Thus it is consistent with our seeing that systematically higher tropopause altitudes, as implied by Wirth's upper troposphere relative vorticity concept, occur when the station lies south of the jet, and lower, but more variable tropopause altitudes occur when the station is north of the jet. This motivates our future plans to run very high resolution Held/Suarez-type GCMs to see what horizontal and vertical resolutions are necessary to resolve the filamentary mixing that leads to high vertical PV gradients at the extratropical tropopause.

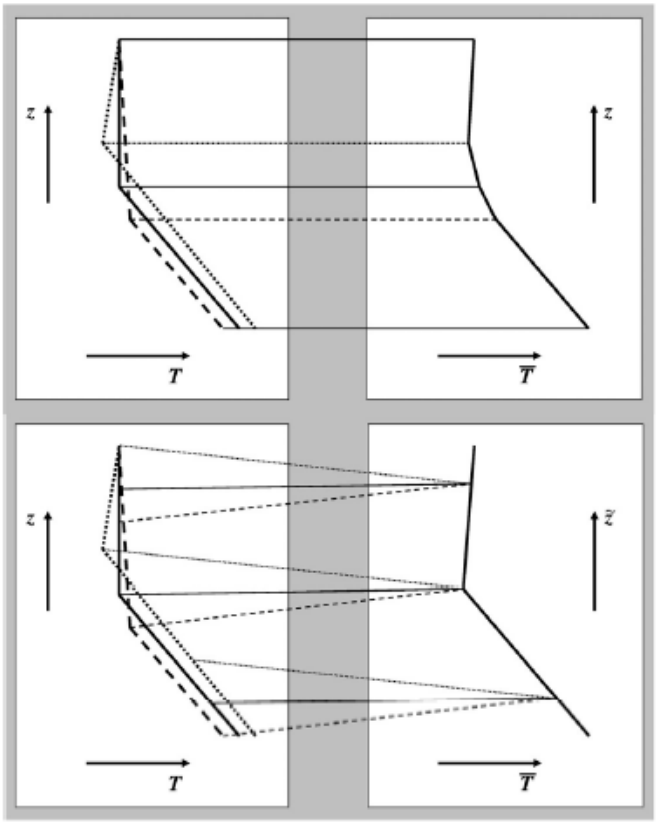

Fig. 1.1 — Figure 1 from Birner (2006). The top panel depicts an averaged sounding (right) taken from three hypothetical temperature soundings (left) when averaged with respect to a constant geophysical reference level (typically the ground or sea-level pressure). The bottom panel is averaged from the same three hypothetical temperature soundings (left) to create an average profile (right) except the tropopause is the geophysical reference level. Note that the tropopause maintains a sharper transition from tropospheric to stratospheric characteristics in the profile averaged with respect to the tropopause.

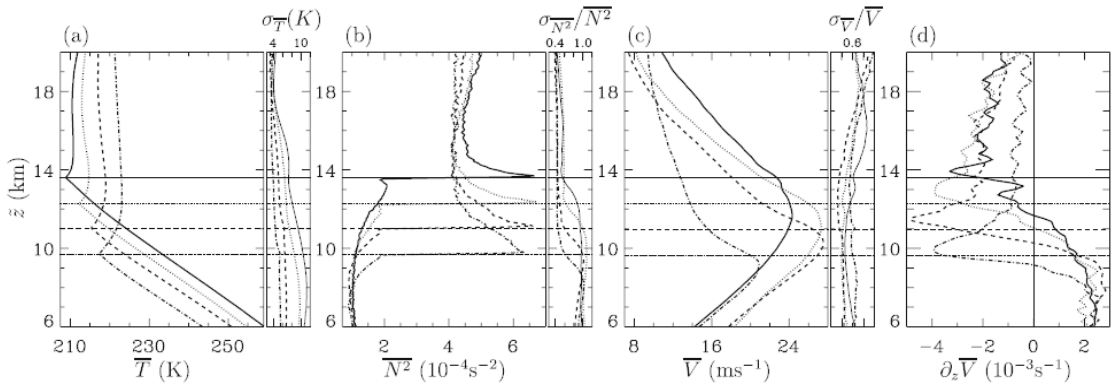

Fig. 1.2 — Figure 3 from Birner (2006) presenting annual climatologies for (a) temperature, (b) buoyancy frequency squared, (c) horizontal wind, and (d) the vertical shear of the horizontal wind for four West Coast stations: Miramar NAS, CA (solid), Reno, NV (dotted), Quillayute, WA (dashed) and Yakutat, AK, (dash-dotted) with horizontal lines denoting the tropopause height for each respective station.

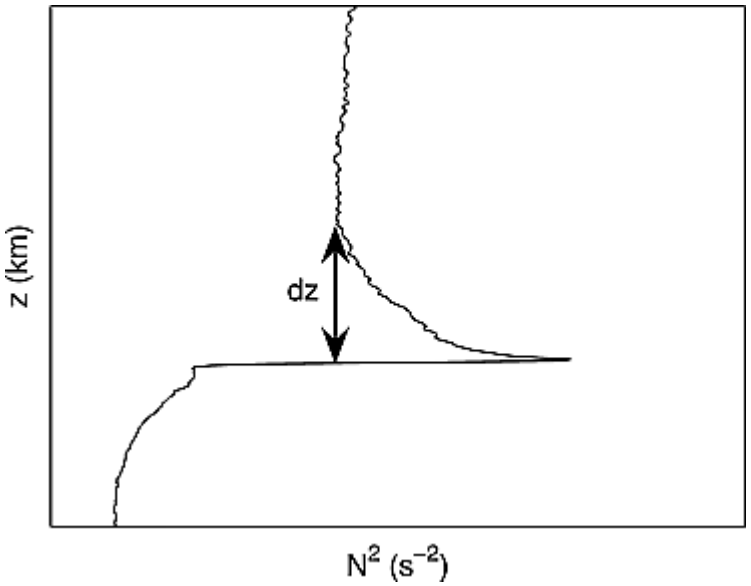

Fig. 1.3 – Schematic illustrating the definition of the ESTL (from Bell and Geller, 2008, dz= ESTL)

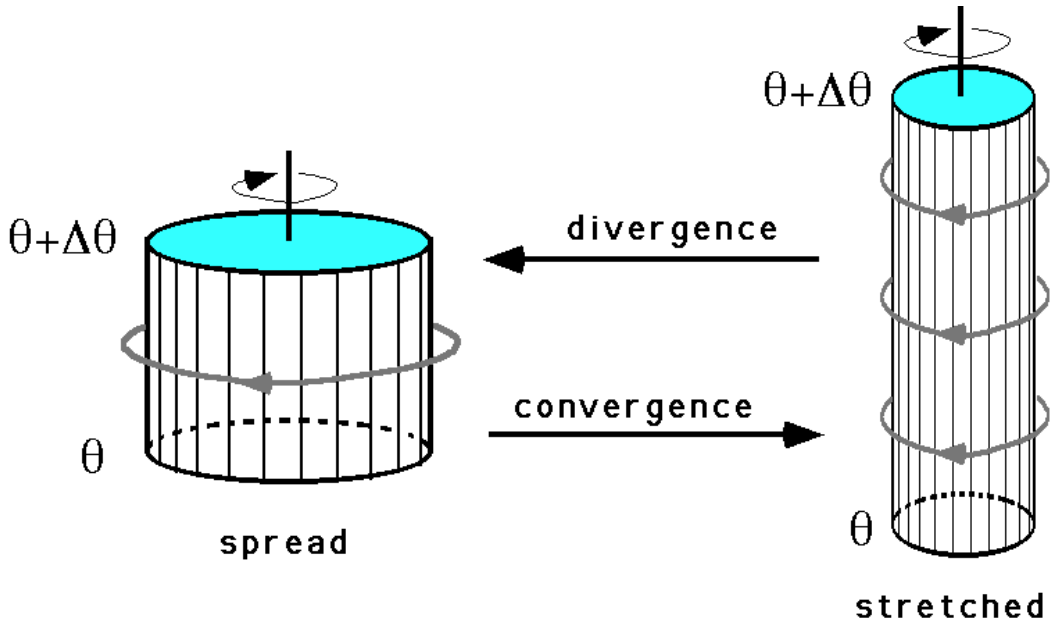

Figure 1.4 — Conservation of potential vorticity. The potential temperature of the bottom and the top of the column remain unchanged during spreading and stretching. (Figure 4 from Potential vorticity and isentropic charts of Geerts and Linacre, 1997)

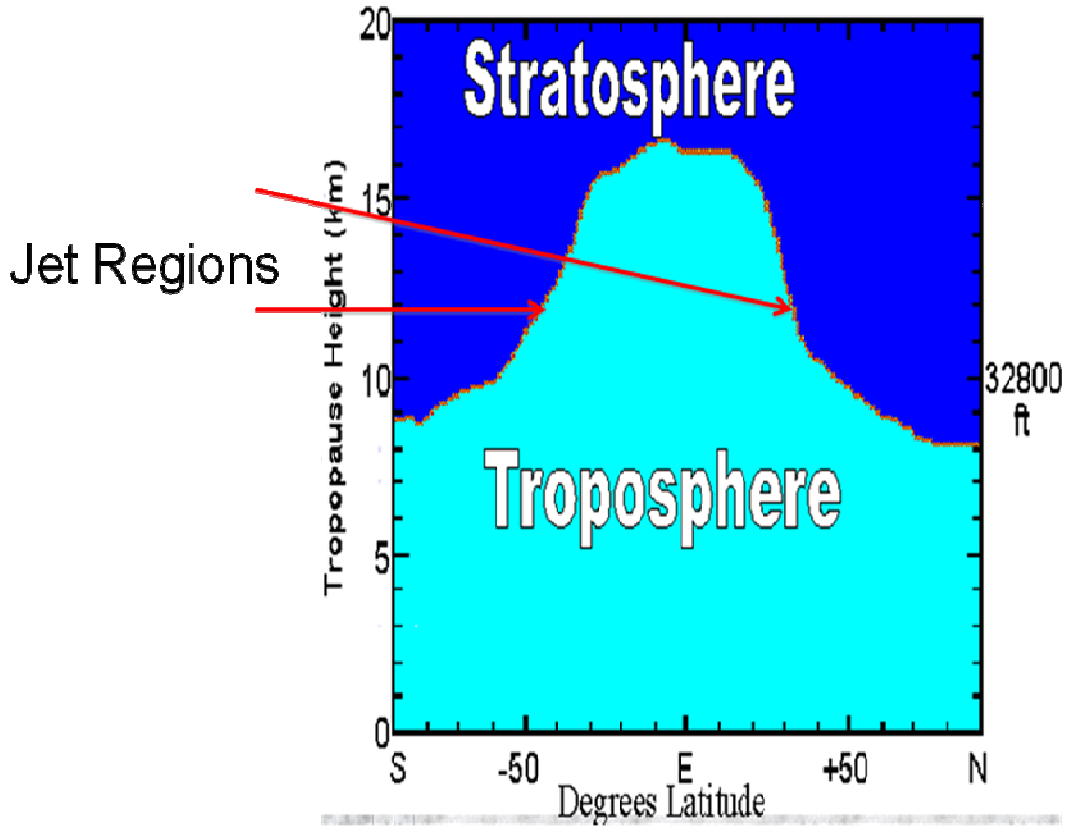

Figure 1.5 – The classical picture of latitudinal tropopause. The red arrows regions are where the jet lies. The tropopause is higher poleward and lower equatorward for both hemispheres. (Figure adapted from Geerts and Linacre, 1997)

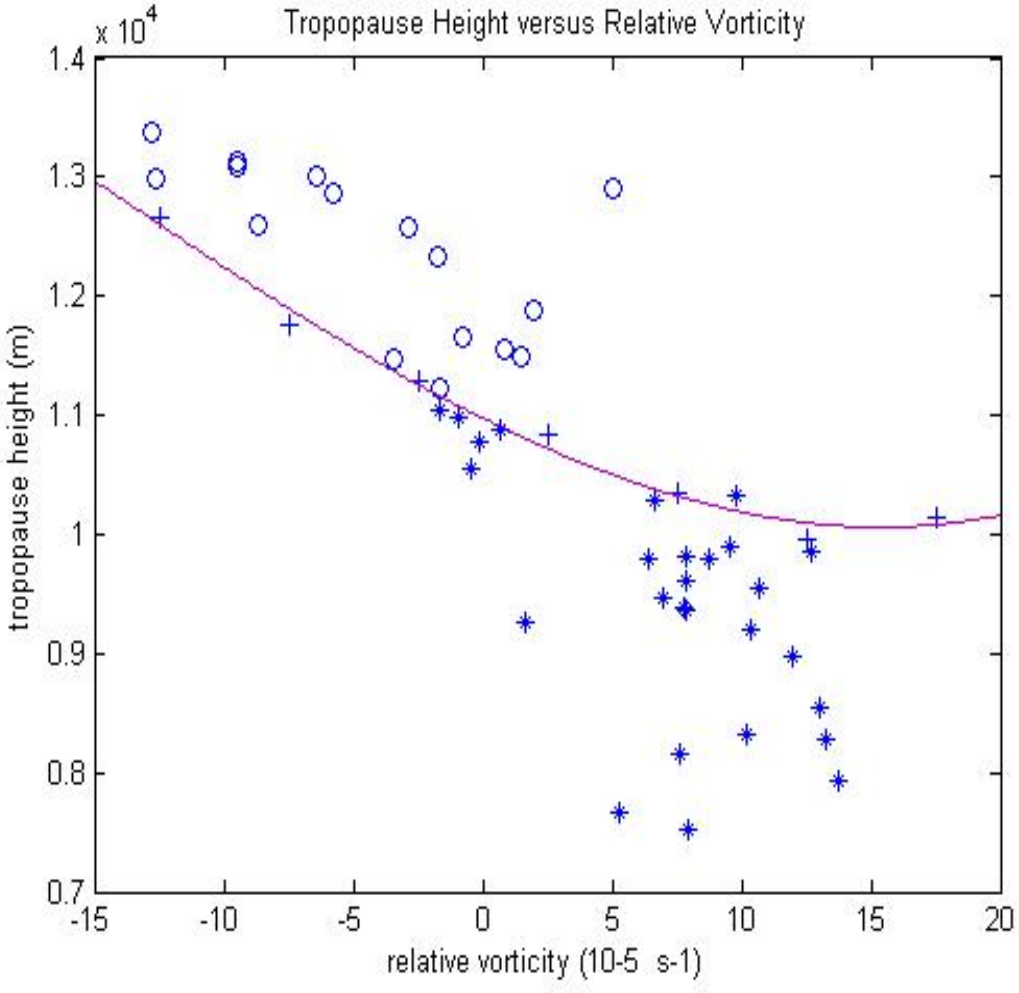

Fig 1.6 – Tropopause height (m) versus relative vorticity (10^{-5} s^{-1}) at 200 hPa for Dodge City from December, 2003 to February, 2004. Plus signs are the average of tropopause height and the curve is the best-fit to the average tropopause height within each relative vorticity bin. Circles (Stars) are individual cases where Dodge City is south (north) of the jet.

2. Methodology

2.1 Data Sets and Description of Data

Three data sets have been used in the analysis involved in this project. The dataset used in our investigation of the extratropical tropopause structure as a dry baroclinic wave passes through is the standard radiosonde data set. The high resolution radiosonde data set is used to double check the height of the tropopause given by the standard radiosonde data set. The upper tropospheric relative vorticity was obtained from the gridded data from NARR (North American Regional Reanalysis) products.

2.1.1 Standard Radiosonde Data Set

Radiosondes have been launched once or twice daily globally since 1940's. The original purpose of reducing the data transmitted for vertical soundings was to make the data rapidly accessible in the days when there were not yet capabilities for large data storage and rapid communication of large amounts of data. The protocol is to have soundings report the so-called mandatory pressure levels which are 1000, 925, 850, 700, 500, 400, 300, 250, 200, 150, 100, 70, 50, 30, 20, and 10 hPa depending on the final altitude reached. These levels are designed so that there are the same constant pressure surfaces reported independent of station and region. Significant and additional levels are also reported and are defined by the Federal Meteorology Handbook (OFCM 1997). These include the surface, the tropopause and the highest level achieved, etc. The significant levels based upon changes in the linearity of the thermal profile intrinsically include the tropopause, but it is a derived level based upon the WMO thermal tropopause criterion.

Although a substantial number of levels are provided in the lower atmosphere, the resolution given by the standard radiosonde data set is still coarse. However, one can interpolate the standard radiosonde data set to a resolution comparable with the high resolution data set and maintain information on the fine-scale nature of the tropopause region, thus we still can see the clear inversion layer and sharpness around the tropopause (Bell and Geller, 2008). The standard soundings used in this thesis were obtained from IGRA (Integrated Global Radiosonde Archive), and this data set freely is available to all without modification. An analysis of the standard radiosonde data set obtained through IGRA (available at http://www.ncdc.noaa.gov/oa/climate/igra/) was performed using a cubic-spline fit to interpolate the standard radiosonde profile to the same 30 meter vertical resolution as the high resolution data set.

2.1.2 High Resolution Radiosonde Data Set

The high resolution data set is freely available from the SPARC (Stratospheric Processes and their Role in Climate) Data Center (www.sparc.sunysb.edu). The SPARC initiative is part of the World Climate Research Program. Use of high-resolution radiosonde for gravity wave analysis was pioneered by Allen and Vincent (1995) using high resolution radiosonde observations over Australia to study temporal and spatial variations of gravity wave activity in the lower atmosphere. The high resolution radiosonde data contained at the SPARC Data Center consists of data from 93 U.S. operated upper-air observing stations from 1998 to 2008. The radiosonde thermistor, hygristor, pressure sensor, and balloon tracking radiotheodilite information using the

MicroArt system give measurements of temperature, humidity and pressure. The meteorological data are transmitted as 6 second averages and the tracking data are also transmitted every six seconds. The typical ascent rate of these balloons is approximately 5 m/s in the troposphere and lower stratosphere, which leads to a vertical resolution of approximately 30 meters. The National Weather Service is currently implementing the Radiosonde Replacement System (RRS) at all the U.S. stations. Under this program, during the period 2005-2011 all of the stations will transition to operation with upgraded equipment and with data being archived at 1 second (vertical resolution of ~5 meter) resolution instead of the previous 6 second (~30 meter) resolution. Both 1 second and 6 second resolution data are provided by the SPARC Data Center to users, 1 second resolution data from 2005 to 2008 can be obtained from ftp://atmos.sparc.sunysb.edu/pub/sparc/hres/1_second/ and 6 second data from 1998 to 2008 can be obtained from ftp://atmos.sparc.sunysb.edu/pub/sparc/hres/6_second/. This so-called "high resolution" radiosonde data denotes this higher vertical resolution than is normally supplied. Although the temperature, pressure, and relative humidity information has a vertical resolution of approximately 30 meters in the older system, information on wind speed and wind direction is calculated from differencing the tracking information and this does not have as high vertical resolution. The vertical resolution of the wind data is approximately 150 meters. The cost of obtaining these data has been funded through NSF support, and the data are disseminated through the SPARC Data Center, which has been funded by NASA. The data were obtained originally from the National Climate Data Center (NCDC) as part of their program of archiving the high resolution upper-air data. Figure 2.1 shows the geographical location of the upper-air stations and Table 2.1 lists all of the available stations, their geographical locations and their WMO and WBAN identification numbers. For further information, the reader is referred to the data set documents, which are at the SPARC Data Center http://www.sparc.sunysb.edu/.

2.1.3 Gridded Data Set from NARR

NARR (North American Regional Reanalysis) is a long-term, consistent, high-resolution climate dataset for the North American domain. The major improvements of NARR are in both resolution and accuracy compared to the earlier global reanalysis datasets. In 1977, during the late stages of production of the NCEP-NCAR Global Reanalysis (GR), there was increased attention to regional reanalysis, particularly since the RDAS (Regional Data Assimilation System) is significantly better than the global reanalysis at capturing the regional hydrological cycle, the diurnal cycle and other important features of weather and climate variability. The NARR model uses the very high resolution NCEP Eta Model (32km horizontal resolution and 45 layers) together with the Regional Data Assimilation System which, significantly, assimilates precipitation along with other variables. The improvements in the model/assimilation have resulted in a dataset with substantial improvements in the accuracy of temperature, winds and precipitation compared to the NCEP-DOE Global Reanalysis 2 (http://www.esrl.noaa.gov/psd/data/gridded/data.ncep.reanalysis2.html). NARR currently has output 8 times daily data at 29 levels for most of the variables. The complete list of model output variables can be obtained from NCEP (http://www.emc.ncep.noaa.gov/mmb/rreanl/merged_land_AWIP32.pdf).

The major breakthroughs of the NARR are seen in the precipitation data over the continental United States (CONUS), which is seen to be very near the ingested analyzed precipitation (figure 2.2); fits of tropospheric temperatures and winds to rawinsonde observations; and fits of 2-m temperatures and 10-m winds to surface station observations. The NARR has helped answer questions about the variability of water in weather and climate, in particular as it concerns U.S. precipitation patterns.

Another advantage of the NARR compared to GR is its higher temporal resolution, 3 versus 6 hr. Not only are analyses and first guess fields available at shorter time intervals, but also a considerable fraction of the data are being assimilated at times closer to the observation time. The main reason I chose to use NARR is not only that it is the gridded data set that GEMPAK requires, but also its better resolution.

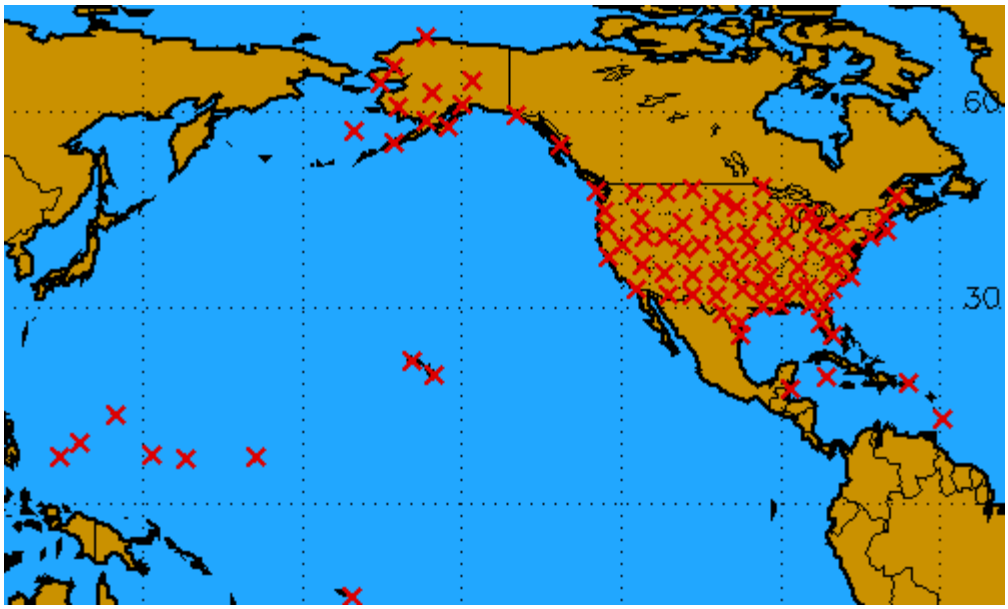

Fig. 2.1 – Location of the U.S. radiosonde sites archived by the high resolution radiosonde data set.

WBAN	Station	State	Country	WMO	Latitude	Longitude	Elevation (m)
3020	SANTA TERESA	NM	US	72364	31.9	-106.7	1257
3160	DESERT ROCK/MERCURY	NV	US	72387	36.62	-116.02	1007
3190	MIRAMAR NAS	CA	US	72293	32.87	-117.15	134
3198	RENO	NV	US	72489	39.57	-119.8	1516
3937	LAKE CHARLES	LA	US	72240	30.12	-93.22	5
3940	JACKSON/THOMPSON FLD	MS	US	72235	32.32	-90.07	91
3948	NORMAN	OK	US	72357	35.23	-97.47	362
3952	N LITTLE ROCK	AR	US	72340	34.83	-92.27	172
3990	FT WORTH	TX	US	72249	32.8	-97.3	196
4102	GREAT FALLS	MT	US	72776	47.45	-111.38	1130
4105	ELKO	NV	US	72582	40.87	-115.73	1608
4106	SPOKANE INTNL APT	WA	US	72786	47.68	-117.63	728
4830	DETROIT/PONTIAC	MI	US	72632	42.7	-83.47	329
4833	LINCOLN-LOGAN COUNTY AP	IL	US	74560	40.15	-89.33	178
4837	GAYLORD / ALPENA	MI	US	72634	44.55	-84.43	448
11501	SEAWELL APT		BA	78954	13.07	-59.5	47
11641	SAN JUAN/ISLA VERDE	PR	US	78526	18.43	-66	3
11813	GRAND CAYMAN		CI	78384	19.3	-81.37	3
11818	BELIZE		BE	78583	17.53	-88.3	5
12842	TAMPA BAY/RUSKIN	FL	US	72210	27.7	-82.4	13
12919	BROWNSVILLE	TX	US	72250	25.9	-97.43	7
12924	CORPUS CHRISTI	TX	US	72251	27.77	-97.5	14
13723	GREENSBORO	NC	US	72317	36.08	-79.95	277
13841	WILMINGTON	OH	US	72426	39.42	-83.82	317
13880	CHARLESTON	SC	US	72208	32.9	-80.03	15
13889	JACKSONVILLE	FL	US	72206	30.43	-81.7	10
13897	NASHVILLE	TN	US	72327	36.25	-86.57	180
13957	SHREVEPORT REGIONAL AP	LA	US	72248	32.45	-93.83	84
13985	DODGE CITY	KS	US	72451	37.77	-99.97	791
13995	SPRINGFIELD REGIONAL AP	MO	US	72440	37.23	-93.4	394
13996	TOPEKA	KS	US	72456	39.07	-95.62	268
14607	CARIBOU	ME	US	72712	46.87	-68.02	191
14684	CHATHAM	MA	US	74494	41.67	-69.97	16
14733	BUFFALO/GRTR ARPT	NY	US	72528	42.93	-78.73	218
14898	GREEN BAY	WI	US	72645	44.48	-88.13	210
14918	INTERNATIONAL FALLS	MN	US	72747	48.57	-93.38	359
14929	ABERDEEN	SD	US	72659	45.45	-98.42	397
21504	HILO	HI	US	91285	19.72	-155.07	10
22010	DEL RIO	TX	US	72261	29.37	-100.92	313
22536	LIHUE/KAUAI	HI	US	91165	21.98	-159.35	36
23023	MIDLAND	TX	US	72265	31.93	-102.2	873
23047	AMARILLO	TX	US	72363	35.23	-101.7	1095
23050	ALBUQUERQUE	NM	US	72365	35.05	-106.62	1619
23062	DENVER/STAPLETON ARPT	CO	US	72469	39.77	-104.88	1611
23066	GRAND JUNCTION	CO	US	72476	39.12	-108.53	1472
23160	TUSCON	AZ	US	72274	32.12	-110.93	788
23230	OAKLAND INT AP	CA	US	72493	37.75	-122.22	6
24011	BISMARCK	ND	US	72764	46.77	-100.75	503
24023	NORTH PLATTE	NE	US	72562	41.13	-100.68	847
24061	RIVERTON	WY	US	72672	43.06	-108.47	1688
24127	SALT LAKE CITY	UT	US	72572	40.77	-111.97	1288
24131	BOISE	ID	US	72681	43.57	-116.22	871
24225	MEDFORD	OR	US	72597	42.37	-122.87	397
24232	SALEM	OR	US	72694	44.92	-123.02	61

25308	ANNETTE ISLAND	AK	US	70398	55.03	-131.57	37
25339	YAKUTAT	AK	US	70361	59.52	-139.67	10
25501	KODIAK	AK	US	70350	57.75	-152.48	4
25503	KING SALMON	AK	US	70326	58.68	-156.65	15
25624	COLD BAY	AK	US	70316	55.2	-162.72	30
25713	ST PAUL ISLAND	AK	US	70308	57.15	-170.22	10
26409	ANCHORAGE IAP/PT. CAMPBE	AK	US	70273	61.17	-150.02	45
26411	FAIRBANKS	AK	US	70261	64.82	-147.87	135
26510	MCGRATH	AK	US	70231	62.97	-155.62	103
26615	BETHEL	AK	US	70219	60.78	-161.8	36
26616	KOTZEBUE	AK	US	70133	66.87	-162.63	5
26617	NOME AP	AK	US	70200	64.5	-165.43	5
27502	POINT BARROW	AK	US	70026	71.3	-156.78	12
40308	YAP ISLAND		KA	91413	9.48	138.08	17
40309	KOROR/PALAU ISLAND		KA	91408	7.33	134.48	33
40504	PONAPE ISLAND		KA	91348	6.97	158.22	46
40505	TRUK INTL/MOEN ISL		KA	91334	7.47	151.85	2
40710	MAJURO/MARSHALL ISL		MH	91376	7.08	171.38	3
41415	GUAM, MARIANA IS		MY	91217	13.55	144.83	111
53103	FLAGSTAFF/BELLEMT (ARMY)	AZ	US	72376	35.23	-111.82	2179
53813	SLIDELL	LA	US	72233	30.33	-89.82	8
53819	PEACHTREE CITY	GA	US	72215	33.35	-84.56	246
53823	BIRMINGHAM (SHELBY APT)	AL	US	72230	33.1	-86.7	178
53829	ROANOKE/BLACKSBURG	VA	US	72318	37.2	-80.41	648
54762	GRAY	ME	US	74389	43.89	-70.25	125
61705	PAGO PAGO INTL ARPT		ZM	91765	-14.33	-170.72	3
92803	MIAMI/FL INTL UNIV	FL	US	72202	25.75	-80.38	4
93734	STERLING(WASH DULLES)	VA	US	72403	38.98	-77.47	85
93768	MOREHEAD CITY/NEWPORT	NC	US	72305	34.7	-76.8	11
93805	TALLAHASEE	FL	US	72214	30.38	-84.37	25
94008	GLASGOW	MT	US	72768	48.2	-106.62	693
94043	RAPID CITY	SD	US	72662	44.07	-103.21	1037
94240	QUILLAYUTE	WA	US	72797	47.95	-124.55	56
94703	BROOKHAVEN	NY	US	72501	40.87	-72.87	20
94823	PITTSBURGH/MOON TOWNSHIP	PA	US	72520	40.53	-80.23	360
94980	OMAHA/VALLEY	NE	US	72558	41.32	-96.37	350
94982	DAVENPORT MUNICIPAL AP	IA	US	74455	41.6	-90.57	229
94983	MINNEAPOLIS	MN	US	72649	44.83	-93.55	287

Table 2.1 – List of stations with high resolution radiosonde data available from the SPARC data center. The column headings are; WBAN identification number, station name, state (if applicable), WMO identification number, latitude, longitude and station elevation in meters.

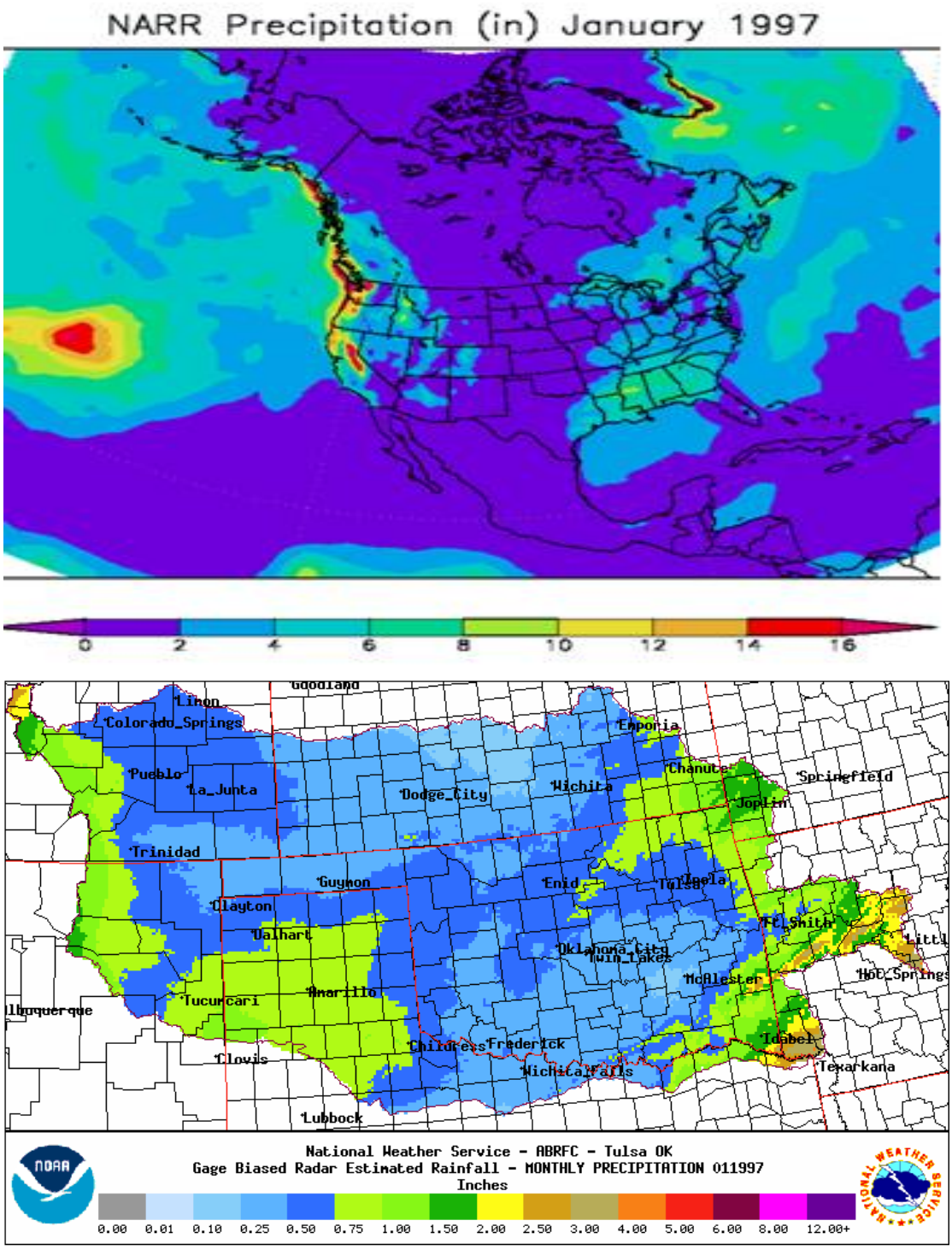

Figure 2.2 – The upper panel is NARR precipitation (inches*10) for January, 1997 and the lower panel is the NOAA precipitation (inches) for the same month.

2.2 Temperature and Stability Profiles Comparisons from the Standard Resolution Radiosonde Data and High Resolution Radiosonde Data

In the dry baroclinic case, standard radiosonde data were used since they have less small-scale variability, thus representing a smoothed version of the high resolution radiosonde data. The 30 meter resolution, produced by interpolation, is used in this study. Data without a tropopause being indicated is excluded (some soundings did not reach the tropopause altitudes). Sometimes, since the report of significant levels might be false, the high resolution radiosonde data were used to double check the correctness of the tropopause height.

The tropopause is calculated via the WMO thermal definition through the high resolution data set. The lapse rate is calculated as a centered difference between two levels, $\Gamma_i=-(T_{i+1}-T_{i-1})/(Z_{i+1}-Z_{i-1})$, where Γ_i is the lapse rate at level i, T is the temperature at levels (single increments in i correspond to altitude increments of 30 meters) i+1 and i-1 (where i is an integer denoting the level of the measurement with i=0 being the surface), and Z is the geopotential height in meters at the same levels as temperature. The lowest level where the lapse rate of the atmosphere is less than 2 degrees/km for at least 2 km above that level is taken to be the tropopause. If the above criterion is not valid (the lapse rate less than 2 degrees/km does not exist for at least 2 km), one searches for the next level above where the criterion is met. Sometimes, multiple tropopauses are found that satisfy the lapse rate criterion. Soundings in which the radiosonde did not reach the tropopause or did not have an identifiable tropopause have been excluded, as have soundings where the balloon did not reach an altitude of at least seven kilometers above the tropopause. If the tropopause height calculated from the high resolution data does not match the tropopause height given by the standard radiosonde data, we examine both the data manually to see if there are unreasonable numbers or miscalculations. We choose the one that seems to be the most correct to determine the actual tropopause height.

The stability or Brunt-Väisälä frequency (N) is convenient for determining whether a level is in the troposphere or the stratosphere, since the stability is greater (larger N) in the stratosphere than in the troposphere. Dry static stability was calculated at 30 meters resolution from the time-averaged soundings, $N^2 = (\Gamma_D - \Gamma_i)\frac{g}{\overline{T}}$, where g is gravity, $\Gamma_D = \frac{g}{c_p}$, c_p is the specific heat at constant pressure, and $\overline{T}$ is the average layer temperature ($\overline{T} = \frac{T_{i+1} + T_{i-1}}{2}$), and $\Gamma_i = -\frac{T_{i+1} - T_{i-1}}{z_{i+1} - z_{i-1}}$. The index level i represents each level of the averaged sounding as integers (non-negative integers if it is the ground-based profile; positive and negative integers (…-2,-1,0,1,2,…) if it is the tropopause-based profile) with 0 being the ground if we are calculating the ground-based stability profile, and with 0 being the tropopause if calculating the tropopause-based stability profile and each positive (negative) integer being one 30 meter level above (below) the ground or the tropopause.

2.3 GEMPAK for Calculation of the Upper Tropospheric Relative Vorticity

GEMPAK, the general meteorology package, is an analysis, display, and product generation package for meteorological data

(http://www.unidata.ucar.edu/software/gempak/). It was developed by NCEP (the National Centers for Environmental Prediction) for use by the National Centers (Storm Prediction Center (SPC), Tropical Prediction Center (TPC), Aviation Weather Center (AWC), Hydrologic Prediction Center (HPS), Marine Prediction Center (MPC), Environmental Modeling Center (EMC), etc.) in producing operational forecast and analysis products. Graphical User Interfaces provide convenient access to interactive data manipulation. A comprehensive set of decoders enables integration of real-time and archive data, products, and bulletins. The GEMPAK distribution consists of a suite of application programs, Graphical User Interfaces (GUIs), meteorological computation libraries, graphic display interfaces, and device drivers for the decoding, analysis, display and diagnosis of geo-referenced and meteorological data.

First, *nagrib* in GEMPAK is used to convert the gridded NARR file to a GEMPAK file. Then, *gdplot* is used with the function *pvor* (calculating the Ertel potential vorticity by the winds from the reanalysis data automatically) or *avor* (calculating the absolute vorticity automatically) to calculate the potential vorticity or absolute vorticity for a rectangular area (in this case, from 35°N to 45°N, and from 120°W to 90°W). The vertical profile (pressure is the vertical axis) of potential vorticity contours for the cross section is plotted by *gdcross*, and the potential vorticity for specific points (stations) is calculated by *gdpoint*. From the PV contours, one can see where the tropopause is sharpening since the level of the 2 PVU surface approximately coincides with the WMO thermal tropopause level in the extratropics. Figure 2.3 is an example. The thermal tropopause derived from the standard radiosonde data in green in figure 2.3 approximates the dynamic tropopause (the 2 PVU surface) derived from the potential vorticity for the cross section from (35°N, 120°W) to (45°N, 95°W). The upper tropospheric relative vorticity can also be determined by subtracting the planetary vorticity (given by the Coriolis parameter, $f=2\Omega\sin\varphi$) from the absolute vorticity.

2.4 Computation of the Distance from the Jet Stream

To objectively examine the correlation between distance from jet and tropopause height, the first thing is to determine the criteria of the range of distances for which the jet has a clear association with the dynamic tropopause height (which is generally close to the WMO definition determined tropopause height, as illustrated in figure 2.3). By comparing the tropopause height and isotachs through the cross-section from (35° N, 120° W) to (45°N, 95°W), we can determine how far the jet association is clearly seen and beyond what distance other influences become apparent. Figures 2.4 and 2.5 show an example. The red line in figure 2.4 shows the region where the dynamic tropopause is sharpening, and the green line shows the region where the dynamic tropopause goes back to its normal height (where the association with the jet stream diminishes and other effects seem to become more important). The blue line in figure 2.5 shows the cross section in figure 2.4, the black square indicates the location where the dynamic tropopause is sharpening, and the pink circle indicates where the jet does not have clear association with the dynamic tropopause height anymore. The perpendicular distance (the red line) from the location where the dynamic tropopause is sharpening (black square) to the jet stream axis (grey line) shows the distance from the sharpened dynamic tropopause to the jet axis for this case, which means the minimum distance that the association with the jet stream exists, whereas the perpendicular distance (the green line) from the location

where the jet association disappears (pink circle) to the jet stream axis (grey line) shows the maximum distance that the jet stream has association with the dynamic tropopause height. Once this range of distance is determined for a given period (2005 winter, December, 2005 to February, 2006), we apply these criteria to another year (2003 winter, December, 2003 to February, 2004) and 3 different stations (Dodge City, Kansas (37.77°N, 99.97°W), Riverton, Wyoming (43.07°N, 108.49°W), and Omaha, Nebraska (41.32°N, 96.37°W)) to examine the jet association with the WMO determined tropopause height.

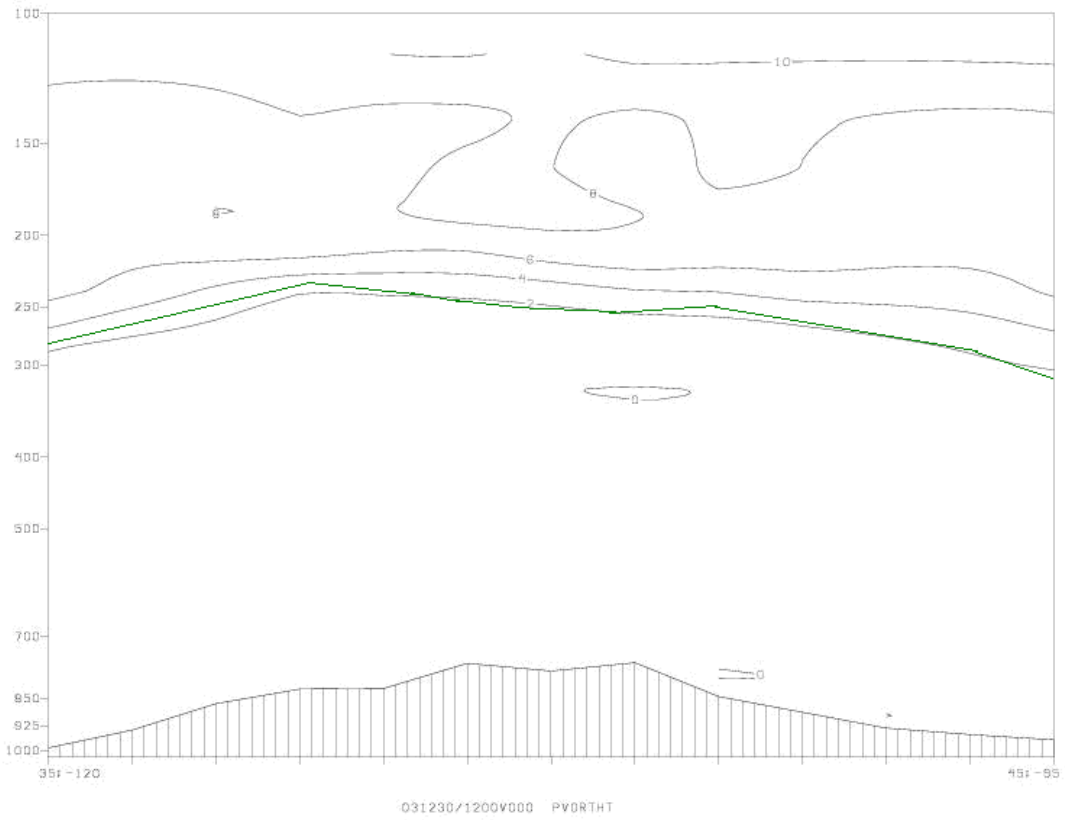

Fig 2.3 – The potential vorticity contours at 12Z, December 30, 2003 for cross section from (35°N, 120°W) to (45°N, 95°W). The 2 PVU line can be taken as the dynamic tropopause. The green line is the thermal tropopause derived from standard radiosonde data.

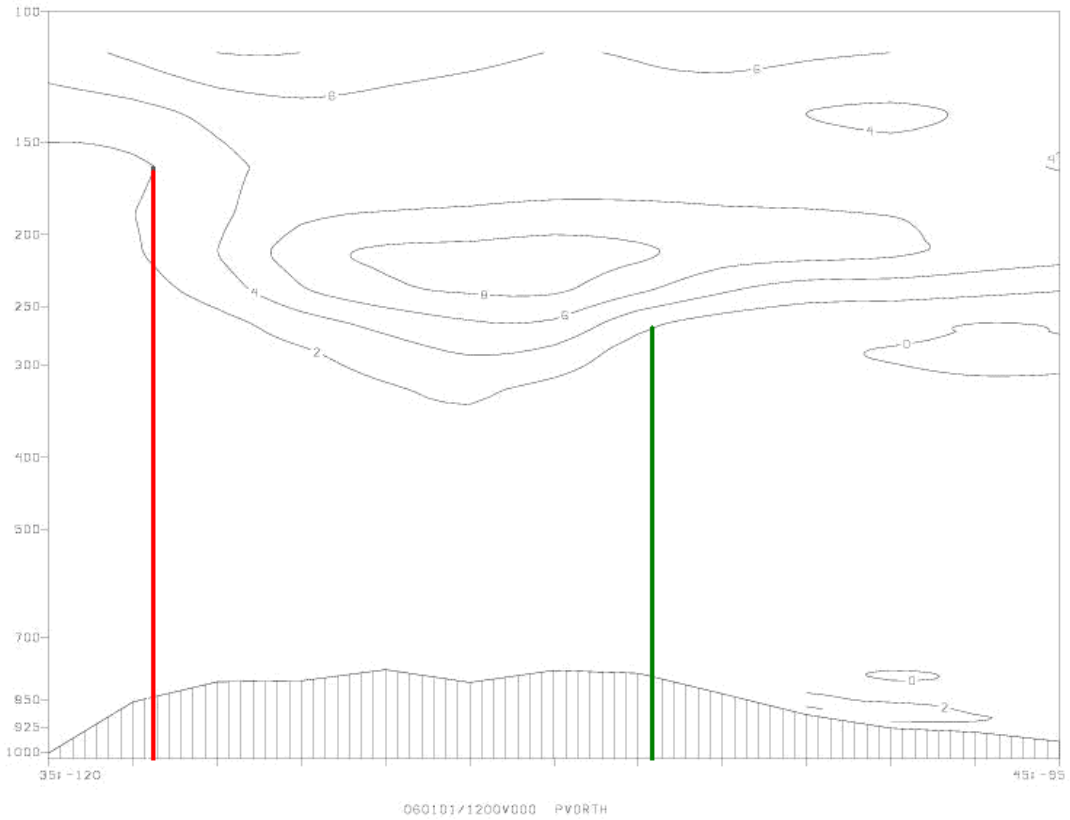

Fig 2.4 – The potential vorticity contours at 12Z, January 1, 2006 for cross section from (35°N, 120°W) to (45°N, 95°W). The 2 PVU line can be taken as the tropopause. The red line shows where the tropopause is sharpening and the green line shows that the tropopause goes back to its normal height.

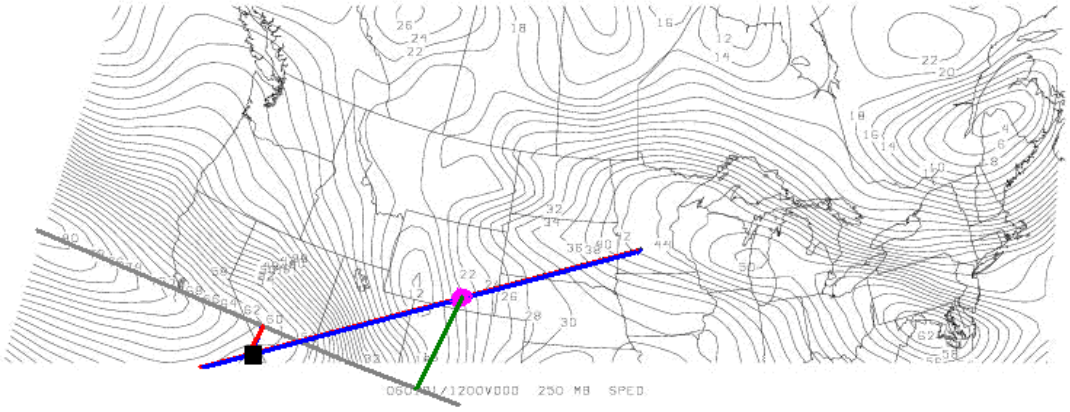

Fig. 2.5 – Isotachs at 1200Z, January 1, 2006 for the United States. The unit for the isotachs is m/s. The blue line is the cross section from (35° N, 120° W) to (45°N, 95°W), the black square is where the tropopause is sharpening, as found in figure 2.3, and the pink circle is where the tropopause goes back to its normal height. The grey line shows the jet stream, the red line indicates the distance from the jet stream to the location where the jet has influence on the tropopause (where the tropopause is sharpening), and the green line indicates the distance from the jet stream to the location where the jet influence disappears.

3. A Case Study of Dry Baroclinic Event in Extratropics

As discussed earlier in the introduction, we believe that baroclinic mixing is the most important factor for the sharpening and lifting of the tropopause in the extratropics. In this work, the pilot case study in the MS thesis of Mr. Shaun Bell (Bell, 2008) is used to visualize how a passage of a dry baroclinic wave lifts and sharpens the extratropical tropopause.

The example case was done for an event that occurred in the Rocky Mountains between December 13 and 19, 2003. The estimated amount of precipitation from east of Rocky Mountains to the Western Great Plains was very small. Most locations had less than five millimeters of rain during the event. We can then assume that there was no, or very little deep convection occurring during this period; that is to say, this was basically a "dry" baroclinic event. Since Juckes (2002) proposed that moist processes can also play an important role in determining tropopause height at mid latitudes, moist processes were excluded by choosing a dry event without active, deep convection occurring.

In this case, we will look into the evolution of the tropopause height and the stability profile with the tropopause as the reference frame.

3.1 Synoptic Setup

The period from December 13 to December 19, 2003 was split into two periods with respect to the passage of the upper level baroclinic wave over the Denver, Colorado upper air station on December 16. The purpose is to see the evolution of the tropopause height and stability profile before and after the wave passage. Figure 3.1 shows the development of the 300 hPa flow for this period. At the beginning of the period, there was a short wave trough diving from the Gulf of Alaska into the Intermountain West. The trough is then amplified as it progressed eastward through the Great Plains around the 16th, and there was a broad scale ridge moving in from the north-west of the North American coast during the latter half of the period.

Standard radiosonde data are used in this case study since there is less small-scale variability (i. e., gravity waves). For each of the three stations (along the cross-line line in figure 3.2, Riverton, Wyoming (43°N, 108°W), Denver, Colorado (39°N°, 104°W), and Dodge City, Kansas (37°N, 99°W) used in this study, the vertical profiles are shown (figure 3.3) to represent the local evolution of the thermal structure of the lower atmosphere at the three stations considered. Denver, Colorado (figure 3.3 (b)), which is the center station among these three stations. Soundings in green are indicative of the passage of the baroclinic wave over Denver Colorado, which is at 12Z, on the 16th. Blue (grey) lines are for 12Z, on the 14th (19th). Thus, the four days "before" and "after" period are chosen with respect to the passage of the wave over Denver, Colorado (the central station along this line). December 13-16 is classified as "before", when the wave has not yet reached the Denver station, and December 16-19 is "after", when the wave has already passed over the Denver station. It can be seen from the time series of the temperature profiles that in the "before" soundings, the tropopause has less of a distinct thermal signature (sharp inversion) than in the "after" soundings. Additionally, a much more distinct inversion is evident just above the tropopause for the "after" soundings (the tropopause inversion layer).

Stability profiles are being plotted as well to see how the ESTL is evolving. The figures are split into two components, the first is the traditional way, using averaging with respect to the ground (Fig. 3.4 (a) and 3.4 (b)), and the second using averaging with respect to the tropopause (Fig. 3.4 (c) and 3.4 (d)). The two different analysis methods show differences in the thermal structure of the tropopause both before and after the wave passage, as might be expected from Birner's results. More striking variations in the thermal and stability structures are seen when tropopause-based averaging is used, however. This shows that even on short times scales, using the tropopause as a geophysical reference level gives a clearer picture than when ground-based averaging is used. The sharp transition from tropospheric to stratospheric stability values just above the tropopause is much stronger when tropopause-based averaging is used. There are large differences in the temperature and stability structures after the wave passage. The tropopause height has increased, in the regions where the baroclinic wave has recently passed through, by approximately 2km regardless of which averaging method is used. In addition to the increase in the height of the tropopause after the baroclinic wave passage, both the vertical gradient of the stability and the maximum of stability at and above the tropopause have also increased. More of the increases in the stability and its vertical gradient are captured when the tropopause-based averaging is used since the changes in the tropopause structure are so variable in time during the wave passage.

Figure 3.3 shows that the tropopause is sharpened and lifted for all three stations. The sharpening and lifting occurred first at Riverton, Wyoming station, as the wave was just passing over Denver, Colorado (vertical profile in green in figure 3.3 (a)). Then this occurred over Denver, Colorado which was just after the wave passage (vertical profile in red following the green line in figure 3.3 (b)). It finally showed up at Dodge City, Kansas station after the wave passed over Denver station (the second vertical profile in red following the green line in figure 3.3 (c)), which is consistent with the passage of the baroclinic wave moving from west to east. Thus, it is quite clear that it is the baroclinic wave that is causing the sharpening and lifting of the tropopause. The same conclusion can be made from the stability profiles since the tropopause is sharpened and lifted after the wave passage (see figure 3.5).

3.2 Conclusions from this Pilot Study

The primary purpose of this pilot study is to explore the response of the extratropical tropopause to the baroclinic wave. From this study of a baroclinic event in the western portion of the country, we see that the Birner method (tropopause-based averaging) is useful for the study of changes in structure during passage of a baroclinic wave even when averages of only four (approximately eight soundings) are being examined. Not only was the thermal structure substantially more apparent in the tropopause-based averages, compared to the ground-based averages, but the sharpness of the tropopause, indicated by both the depth and absolute value of stability in the region just above the tropopause, was also enhanced by averaging with respect to the tropopause. The tropopause was sharpened and lifted after the baroclinic wave passage no matters which averaging method was used (ground- or tropopause-based). This stresses the fact that baroclinic mixing is indeed an important factor in the sharpening and lifting of the extratropical tropopause.

Of course, we are only seeing the changes in the tropopause structure resulting from the baroclinic mixing. The mixing processes themselves are likely being undersampled given the spatial and temporal spacing of the observations.

Besides, figure 3.1 (b), (c), and (d) indicates that there was a trough (cyclonic circulation) passing over the line of the three stations from the 15th to 16th and the lower tropopause height is seen for all stations (see the lines between the blue and green lines in figure 3.3). After the trough passes the line, there came a ridge (anticyclonic circulation) moving into this region and the tropopause was sharpened and lifted. This is consistent with what Wirth has proposed that the sharpness of the extratropical tropopause is greater when the upper tropospheric relative vorticity is anticyclonic.

(a) 12/14/03 00Z (b) 12/15/03 00Z

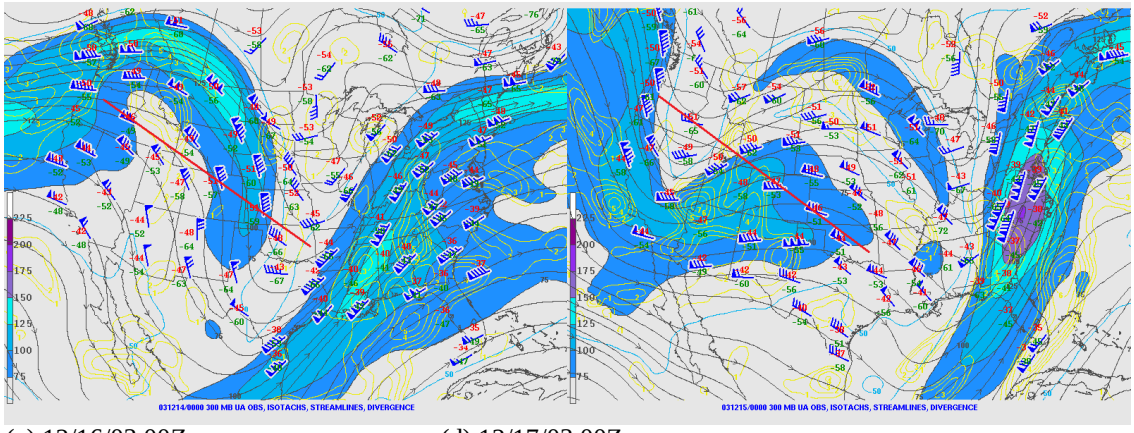

(c) 12/16/03 00Z (d) 12/17/03 00Z

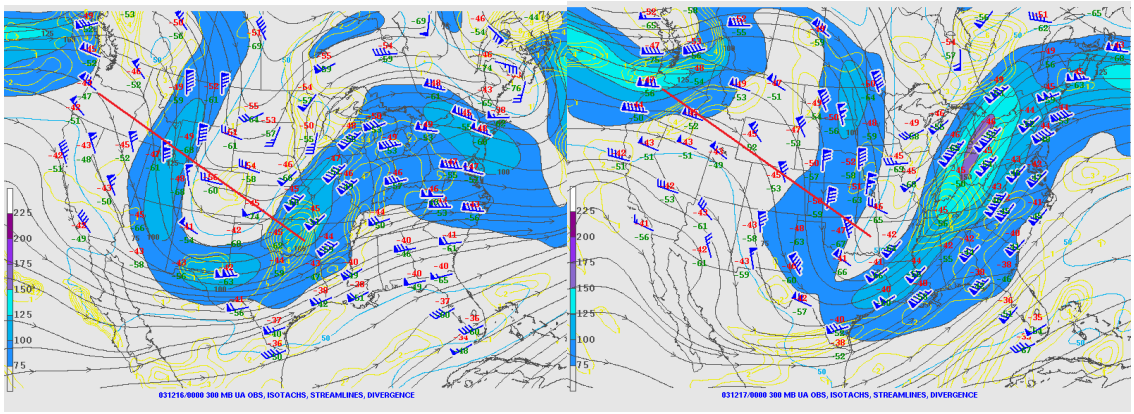

(e) 12/18/03 00Z (f) 12/19/03 00Z

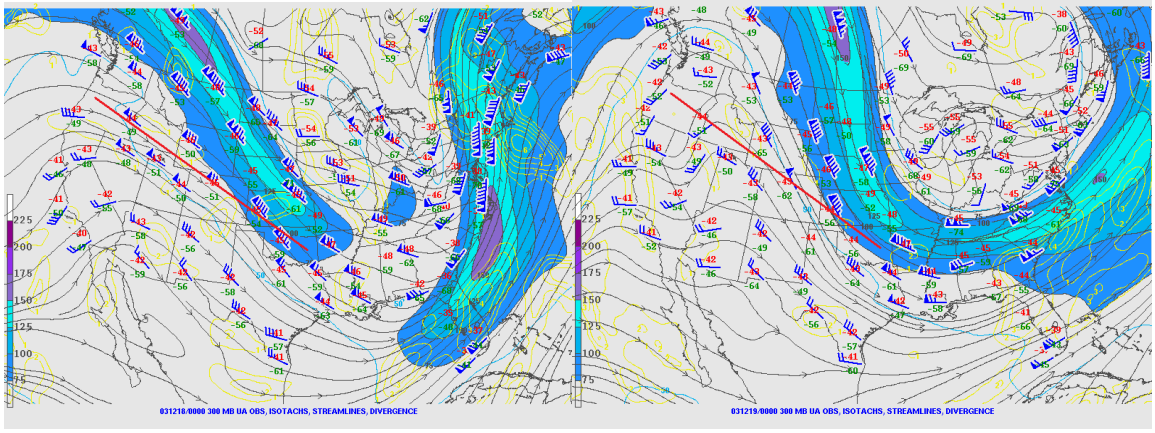

Fig. 3.1 – 300 hPa height (black lines), and isotachs (contoured) daily at 00Z, for the time period, (a) December 13, 2003, (b) December 14, 2003, (c) December 15, 2003, (d) December 16, 2003, (e) December 17, 2003, (f) December 18, 2003. Plots obtained from the Storm Prediction Center's (SPC) operational archive at www.spc.noaa.gov.

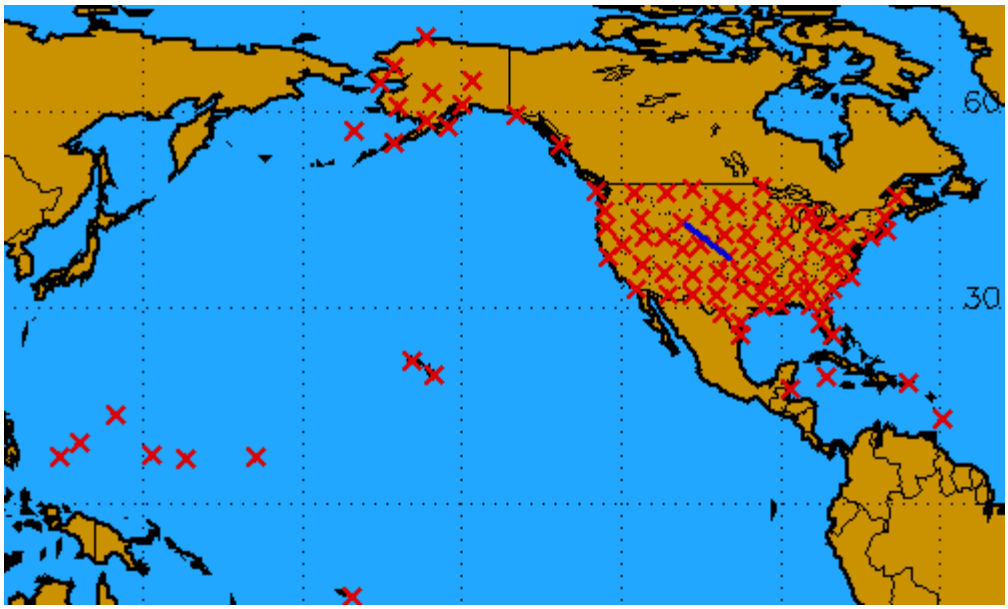

Fig. 3.2 – Map showing approximate regions of cross section used in the pilot case study. The blue line represents the baroclinic cross section centered about the Denver, CO upper air station.

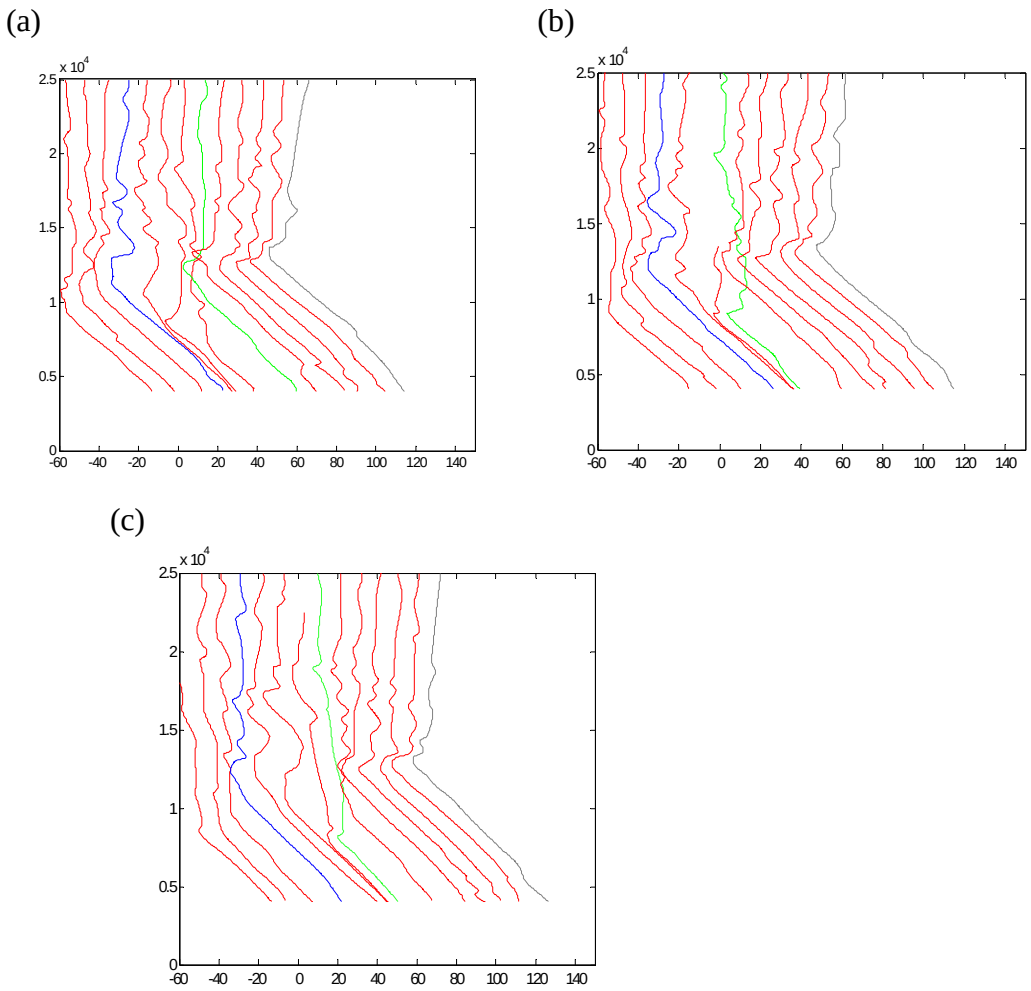

Fig. 3.3 – Time series of sounding profiles from December 13 2003 to December 19 2003 for (a) Wyoming, (b) Colorado and (c) Kansas. The vertical axis is the tropopause height (m) and horizontal is temperature (°C). Temperature is plotted every 12 hours when available and offset by 10 degrees for each successive time. Soundings in green are indicative of the passage of the baroclinic wave over Denver, Colorado, which is at 12Z on the 16th. Blue (grey) lines are for 12Z on the 14th (19th).

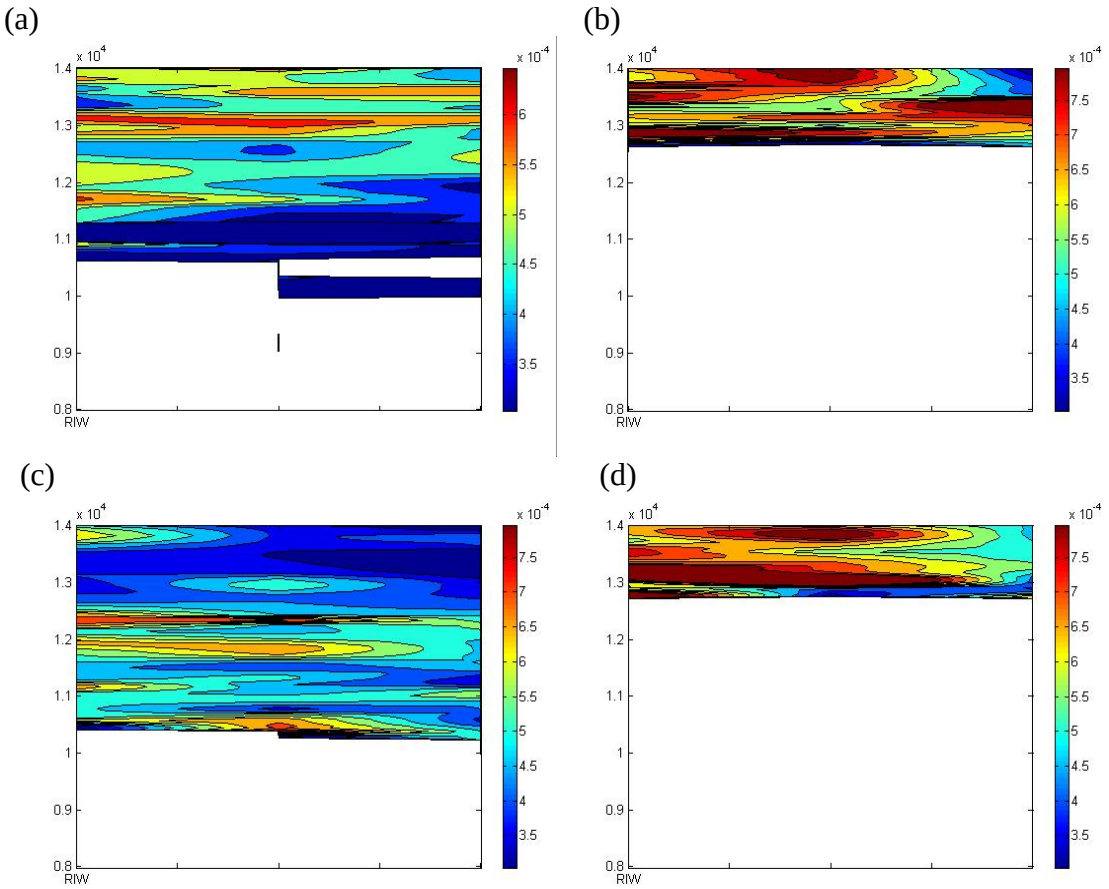

Fig. 3.4 – Contour plots of stability (N^2) averaged before the passage of the baroclinic wave (December 13-16, panels (a) and (c)) and after the passage (December 16-19, panels b and d). The vertical axis is stability (s^{-2}) and horizontal is the three stations from east to west, Wyoming, Colorado, Kansas. The panels (a) and (c) are averaged with respect to the ground and panels (c) and (d) are averaged with respect to the tropopause. Values less then $3x10^{-4}$ s^{-2} which are representative of tropospheric values are not contoured.

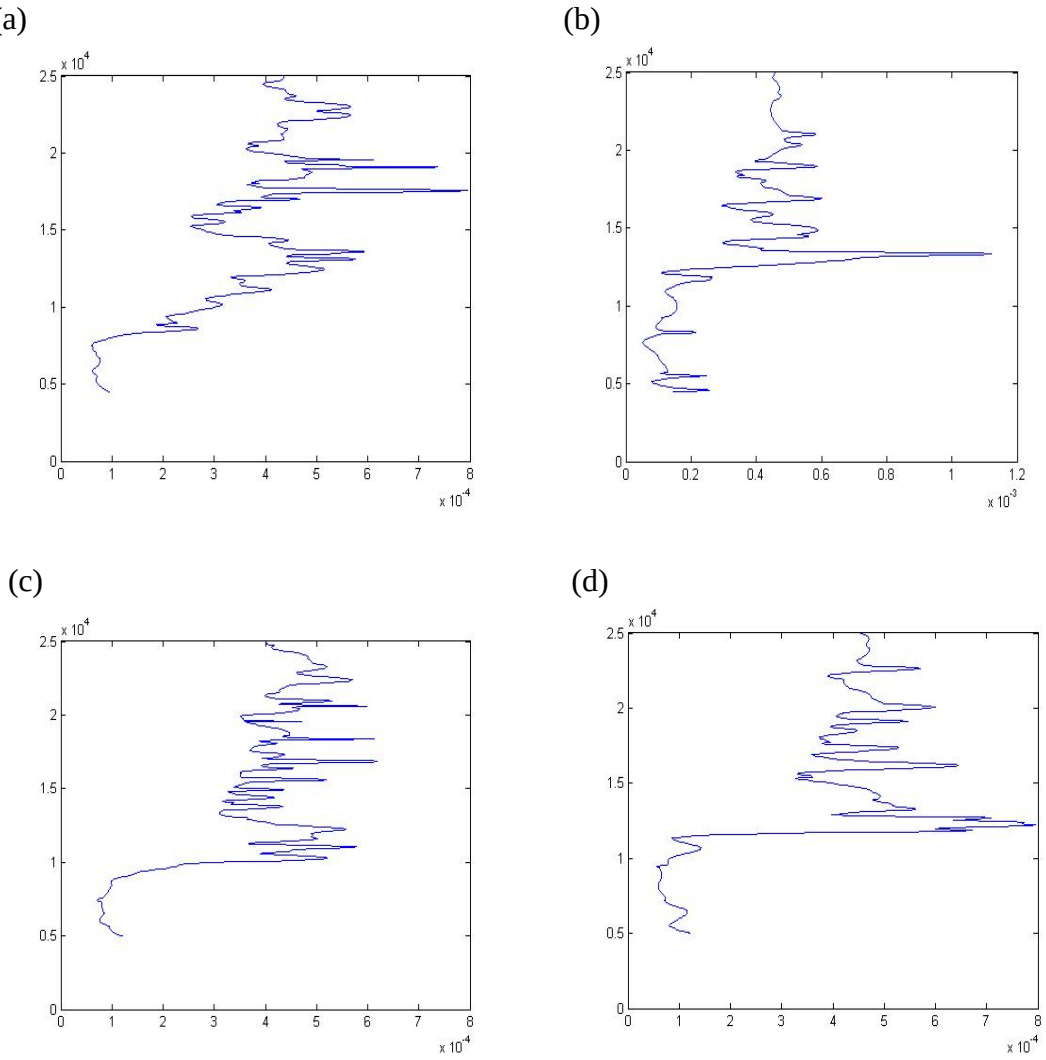

Fig 3.5 – Vertical stability profile for Dodge City. The horizontal axis is stability (N^2) and the vertical axis is height (m). (a) and (c) are before the wave passing over Dodge City. (b) and (d) are after the wave passing over Dodge City.

4. The Association of Distance from the Jet with the Tropopause Height

As mentioned previously, we believe that the distance from the jet is the dominant controlling factor in determining extratropical tropopause height. By comparing the correlation between the distance from the jet and the tropopause height and that between the upper tropospheric relative vorticity and the tropopause height, we will determine which factor is more important in determining the tropopause height.

4.1 Determining the Objective Criteria

A cross-section from (35° N, 120° W) to (45°N, 95°W) is chosen to determine these criteria since there are many stations along that line and this is a region where the jet stream often passes through as synoptic systems move from the Southwest to the Northeast of the United States. Data from the 2005-6 winter are used to determine these criteria. There are 42 realizations used out of 180 possible ones (2 soundings for each day, 90 days from December 1, 2005 to February 28, 2006) where clear jet association with the dynamic tropopause height is seen in the PV cross-sections or in another words, when we can see clear sharpening and lifting of the tropopause accompanying nearby jets, as shown in figure 2.4. The mean station distance for the 42 cases to the location where clear dynamic tropopause sharpening is seen is 195.66 kilometers and the square root of the variance about this mean is 74.50 kilometers. Therefore, we take 121.16 kilometers (subtracting the square root of the variance from the mean) as the minimum distance from the jet, where the jet has clear association with tropopause sharpening, since this will most likely include 84 percent of the cases (assuming a normal distribution). On the other hand, there are 29 data realizations where the station distance from the jet is so large that other factors are seen to be affecting the tropopause, as shown in figure 2.4. The mean distance over which the jet association diminishes and other factors are dominant in affecting the tropopause for these 29 cases is 1507.33 kilometers and the square root of the variance about this mean is 482.69 kilometers. The maximum distance, beyond which the jet association with the tropopause has diminished, is taken to be the sum of the square root of the variance and the mean, which is 1990.02 kilometers.

Once these criteria are decided upon, we can start to look into different stations in different years to examine the correlation between the distance from the jet and the tropopause height. The distances from the jet stream that will be included in our study are within the range between 121.16 to 1990.02 kilometers. Distances from the jet stream which are larger than this maximum distance from the jet or smaller than this minimum distance from the jet are not considered.

4.2 Correlation between the Distance from the Jet and the Tropopause Height

Three stations, Dodge City, Kansas; Riverton, Wyoming; and Omaha, Nebraska during the 2003-4 winter (December, 2003 to February, 2004), are chosen for study here. These stations in the middle United States have been chosen randomly since the jet association should exist everywhere as long as there are jet passages in the region and period we have selected. A different winter from that used to determine the minimum-maximum jet distance criteria is utilized in this study so that our analysis is not dependent on a particular winter's behavior.

There are 34, 49, and 43 cases that meet our criteria for Dodge City, Riverton, and Omaha, respectively. Figure 4.1 shows the comparisons of the relationship between the distance from the jet and the tropopause height and also that between the upper relative vorticity and the tropopause height for these three stations. The horizontal axis represents the case number. These three variables (tropopause height, distance from the jet, and upper relative vorticity) have been normalized to the same units by dividing each of their deviations from its mean by the corresponding square root of the variance. The vertical axis represents the values of the three normalized variables. The blue lines are the variations in the tropopause height for the identified jet events, the red line is for the distance from the jet, and the purple one is for the upper tropospheric (200 hPa) relative vorticity. Not much difference between the 2 correlations (one being between the distance from the jet and the tropopause height; the other one being between the upper tropospheric relative vorticity and the tropopause height) for Dodge City can be seen. The red line correlates better with the blue line than does the purple line for the other two stations (Riverton and Omaha), which indicates that the station distance from jet stream has higher correlation with the tropopause height than does the upper tropospheric relative vorticity does for these two stations. This can be seen from calculations as well (Table 4.1 and 4.2). The two correlations are statistically similar to each other for Dodge City and it is also true at 95% interval of correlations. For the other two stations (Riverton and Omaha), the interval of 95 % confidence limit of correlation between the distance from the jet and the tropopause height sits at higher band than that between the upper tropospheric relative vorticity and the tropopause height. The differences between the two correlations are larger than at Dodge City, but they are still not significant at ±1 sigma level. These results are not unexpected, given that the "distance from the jet" is highly correlated with the upper troposphere relative vorticity. Thus, we now calculate the partial correlations, which correspond to the correlation of one of these factors with the other held constant (see Statistical Methods In the Atmospheric Sciences by Wilks, DS, 2005).

The partial correlation between the distance from the jet and the tropopause height, which corresponds to holding the upper tropospheric relative vorticity fixed, gives a higher value than that between the upper tropospheric relative vorticity and the tropopause height, which corresponds to holding the distance from the jet stream fixed (see Table 4.3) for Riverton and Omaha. Taking the correlation coefficient squared to be indication of the explained variance, we see that for Omaha, the partial correlation with the distance from the jet explains more than 50% 0f the variance, while the upper tropospheric relative vorticity only explains less than 25%. For Riverton, the corresponding numbers are more than 45% for the distance from the jet, while for the upper troposphere relative vorticity it is less than 30%. The amount of the total variance explained by these two factors are similar to each other for Dodge City, although even for this station the percent of the explained variance is slightly larger for the distance from the jet than for the upper troposphere relative vorticity. These results are consistent with our hypothesis that the distance of the station from the jet stream is more important in determining the tropopause height than is the upper troposphere relative vorticity at the two northern stations, but the factors seem equally important at Dodge City.

4.3 Some Conclusions from this Correlation Study

It is shown from both the plots and calculations for the two northern stations that the distance from the jet stream has higher partial correlation with the tropopause height than does the upper tropospheric relative vorticity. However, the value of the correlation between the distance from the jet stream and the tropopause height seems to be close to that between the upper relative vorticity and the tropopause height for Dodge City, and also both values are higher compared to those from the other two stations. We assume that the location of the station might be the reason causing these correlation values to not only be close to each other, but also be relatively high. Dodge City is the most southern station among these three. Table 4.4 shows that the mean distance from the jet stream when Dodge City is south (north) of the jet stream is the largest (smallest) among these three stations. We can see from figure 4.2 that when the station is sufficiently far south of the jet stream, the correlation is higher and more stable (the red circle region); whereas, if the station is near the blue circle region (closer to the jet stream, but still beyond the minimum distance criteria (121.16 km) where the jet has clear association with the tropopause height. In these cross-sections, the distance scale is divided by 84 small rectangular segments (the rectangles under the figures of the cross-section of potential vorticity contours) and 1 rectangle is around 30 km in distance. Thus, since Dodge City has the largest mean value of the distance from the jet stream when that station is south of the jet, the correlation between the distance from the jet stream and the tropopause height should be the highest when the station is south of the jet, as shown in table 4.6. The same reasoning can be seen when the stations are north of the jet. Because Riverton has the largest mean value of the distance from the jet stream when the station is north of the jet and has the largest fraction of the total cases studied when the station is north of the jet, it has the highest correlation between the tropopause height and the distance from the jet when north of the jet. However, as shown earlier by Neilsen-Gammon (2001) there are less small-scale filamentary structures equatorward than poleward of the jet. Thus the correlations are lower for all three stations when they are north of the jet than south of the jet. These filamentary structures will have less influence on the southern most station. Since Dodge City is the most southern station and it has the smallest mean value of the distance from the jet stream when the station is north of the jet, it is reasonable that its distance from the jet stream has the highest correlation with the tropopause height. Figure 4.3 shows that Dodge City is at the flat region (the correlation is higher and more stable) when south of the jet, and at the slope area when north of the jet (the correlation is not that clear). Also, the cross-section where Dodge City is at the center in figure 4.5 are 3 cases among the 9 (figure 4.4) for which Dodge City is south of the jet. They show that Dodge City is closer to the flat region (the red circle area) than the slope region (the blue circle area). We believe that this might explain why the value of the correlation between the distance from the jet and the tropopause height for Dodge City is the highest among the three stations selected for study here.

Figure 4.6 shows the average tropopause height within each vorticity bin for 3 stations in this study and the cases which jet has clear association with the tropopause height in 2003-4 winter. The average tropopause height is higher when the upper tropospheric relative vorticity is negative (anticyclonic circulation); lower when the vorticity is positive (cyclonic circulation) for all stations in study, which corresponded to Wirth's arguments. The cases where the jet has clear association with the tropopause

height for Dodge City still show that the tropopause is higher when upper tropospheric circulation is anticyclonic and lower when it is cyclonic. However, the Riverton and Omaha cases do not show clear correlation between the tropopause height and the upper tropospheric relative vorticity. Although for the cases when Riverton is north of the jet, the correlation that the tropopause height is lower when the upper circulation is more cyclonic can be seen, the cases where Riverton is south of the jet are not consistent with Wirth's hypothesis. The correlations for both the cases where Omaha is north and south of the jet are not that clear as well. The correlation between the upper tropopheric relative vorticity and the tropopause height seem higher when the upper circulation is anticyclonic than cyclonic circulation (figure 4.7). Dodge City is closer to the "high-correlated" region since it is the south most station which has the highest chance of anticyclonic circulation might also explain the highest correlation it has between the upper tropospheric relative vorticity and the tropopause height among the three stations (table 4.7). Furthermore, these results are consistent with our previous calculations that showed the correlation between the tropopause height and the upper tropospheric relative vorticity is not as high as for these stations as for Dodge City. This corresponds to our hypothesis that the distance from the jet is more important in determining the tropopause height than is the upper tropospheric relative vorticity, especially for northern stations.

(a) Dodge City, Kansas

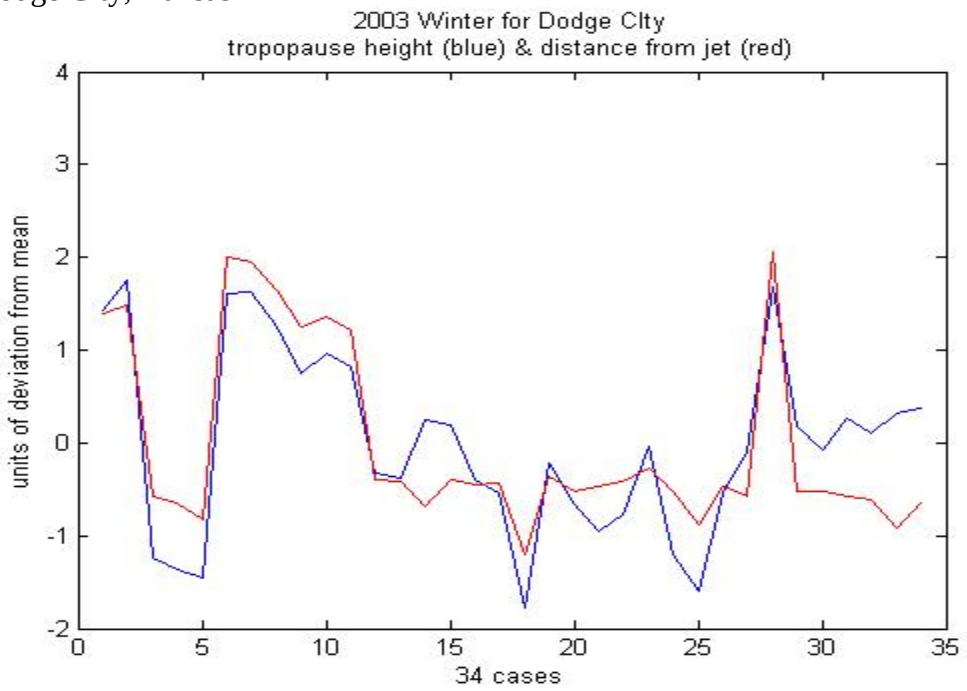

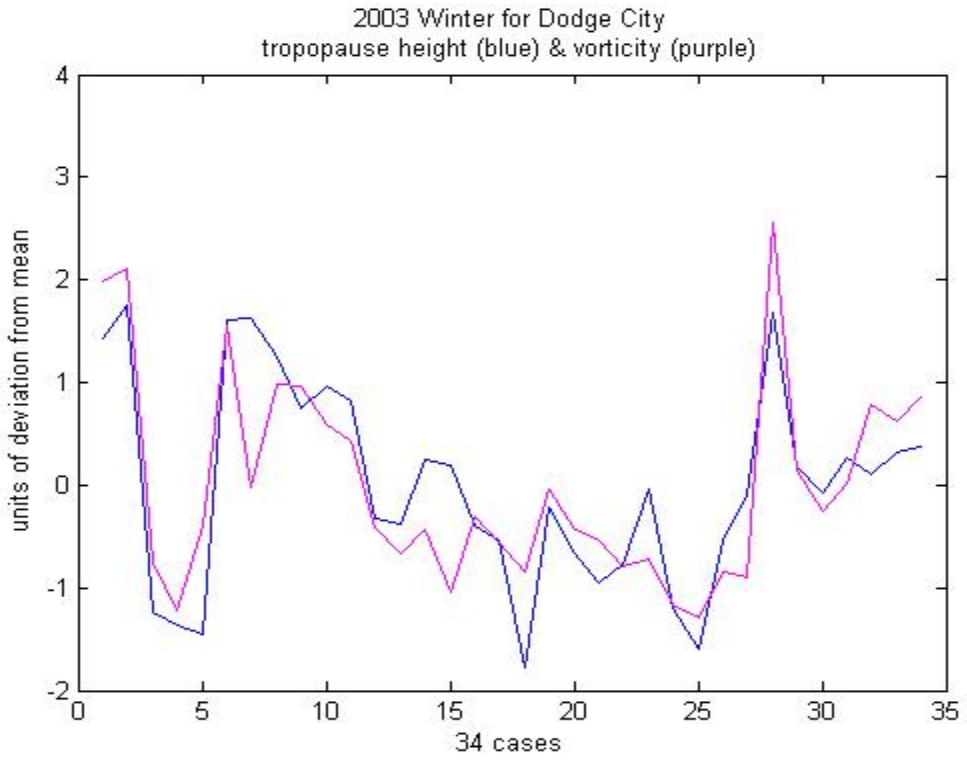

(b) Omaha, Nebraska

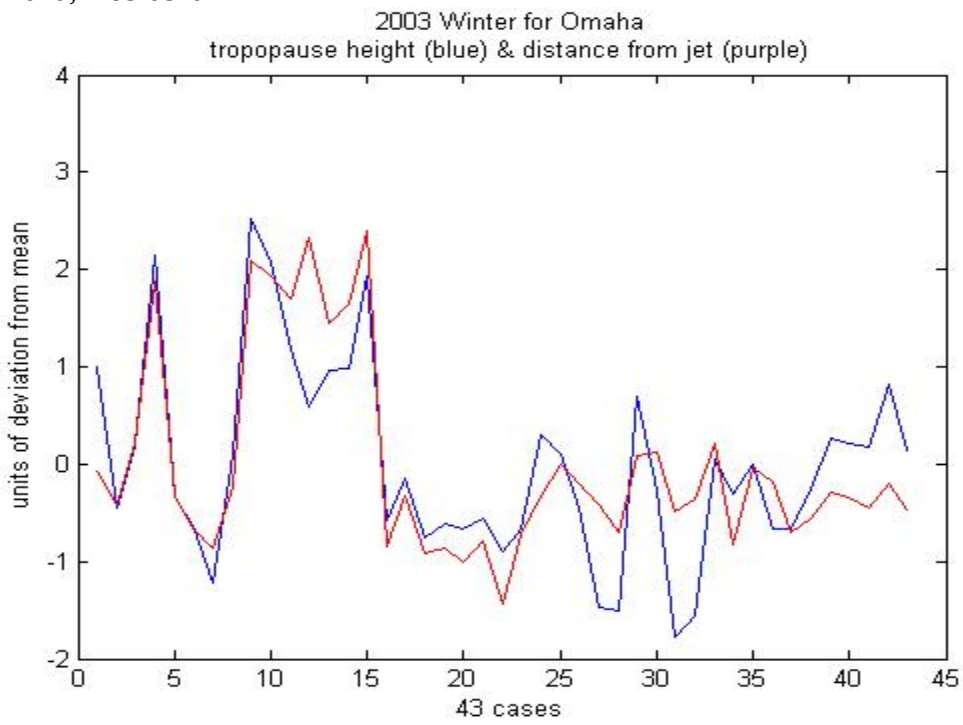

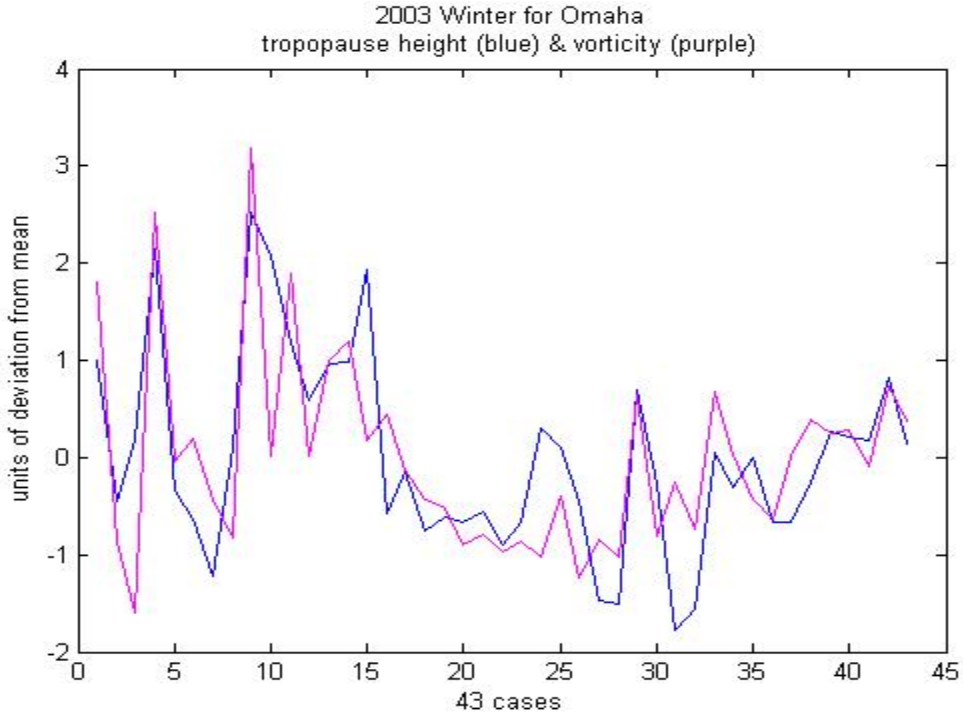

(c) Riverton, Wyoming

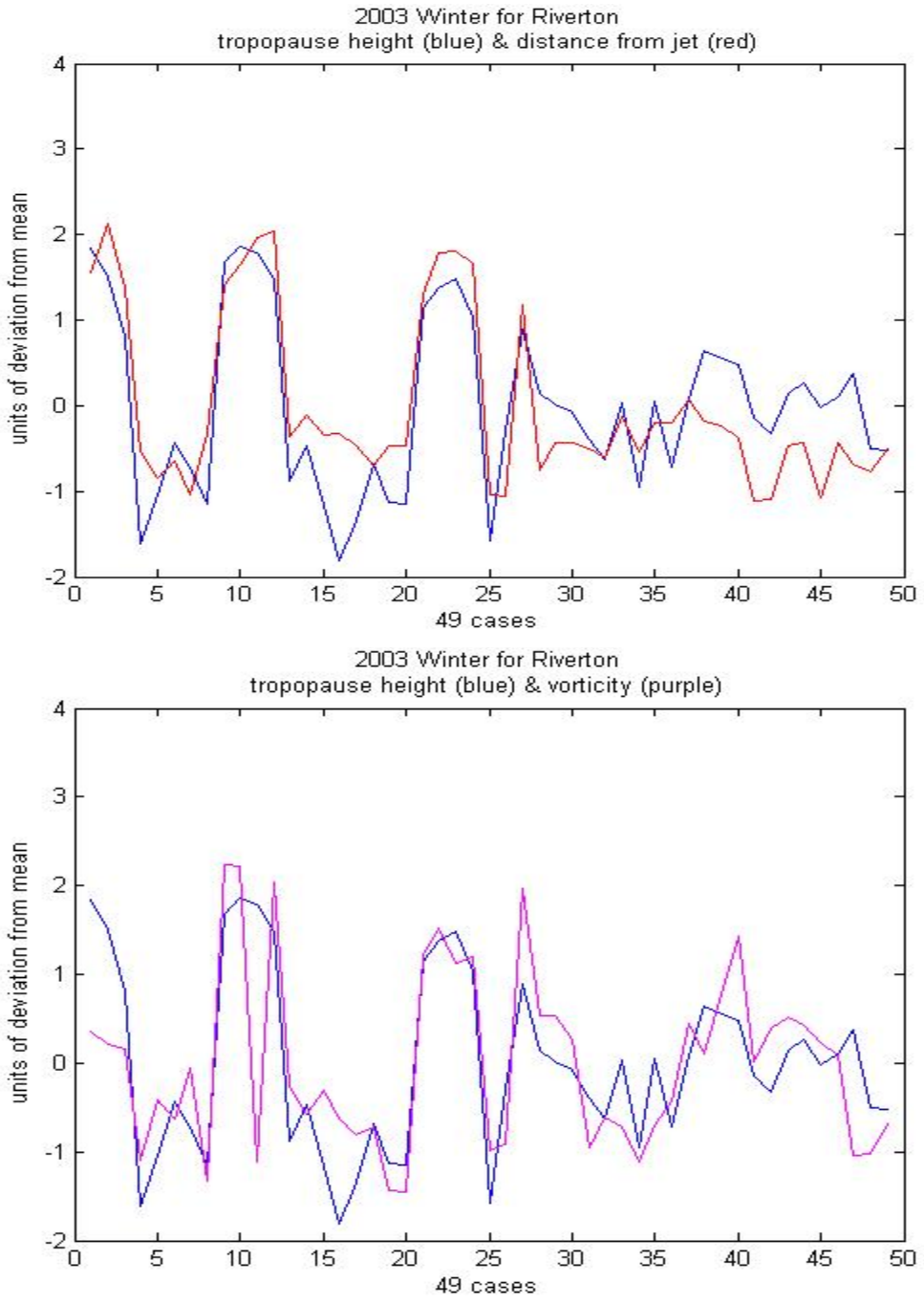

Figure 4.1— Relation between the distance from the jet (red) and the tropopause height (blue) and that between the upper relative vorticity (purple) and the tropopause height for (a) Dodge City, (b) Omaha, and (c) Riverton.

	Dodge City	Omaha	Riverton
Distance from jet	0.85±0.094	0.82±0.086	0.81±0.09
Upper tropospheric relative vorticity	0.83±0.098	0.71±0.10	0.73±0.11

Table 4.1 – The correlation between the tropopause height with each variance (distance from jet and upper tropospheric relative vorticity) for 2003-4 winter (December, 2003 to February, 2004) at Dodge City, Kansas, Omaha, Nebraska, and Riverton, Wyoming. The values followed by ± are one standard deviation.

	Dodge City	Omaha	Riverton
Distance from jet	0.71~0.92	0.68~0.90	0.68~0.89
Upper tropospheric relative vorticity	0.69~0.91	0.52~0.83	0.56~0.84

Table 4.2 – 95% confidence interval for correlations between the distance from jet and tropopause height and that between upper tropospheric relative vorticity for Dodge City, Kansas, Omaha, Nebraska, and Riverton, Wyoming.

	Dodge City	Omaha	Riverton
Distance from jet	0.61	0.71	0.68
Upper tropospheric relative vorticity	0.57	0.49	0.53

Table 4.3 – The partial correlation between the tropopause height with each variance when the other one is fixed for 2003-4 winter (December, 2003 to February, 2004) at Dodge City, Kansas, Omaha, Nebraska, and Riverton, Wyoming.

	Dodge City	Omaha	Riverton
South of the Jet Stream	1264 km	775 km	750 km
North of the Jet Stream	853 km	994km	1249 km

Table 4.4 – The mean value of the distance from the jet stream for south and north to the jet stream, respectively for 2003-4 winter at Dodge City, Kansas, Omaha, Nebraska, and Riverton, Wyoming.

	Dodge City (34 cases)	Omaha (43 cases)	Riverton (49 cases)
South of the Jet Stream	9 cases (~26%)	8 cases (~19%)	12 cases (~24%)
North of the Jet Stream	25 cases (~74%)	35 cases (~81%)	37 cases (~76%)

Table 4.5 – The number of cases when the station is south to the jet stream and north to the jet stream, respectively for 2003-4 winter at Dodge City, Kansas, Omaha, Nebraska, and Riverton, Wyoming.

	Dodge City (34 cases)	Omaha (43 cases)	Riverton (49 cases)
South of the Jet Stream	0.76±0.112	0.47±0.143	0.43±0.151
North of the Jet Stream	0.40±0.120	0.52±0.101	0.63±0.103

Table 4.6 – The separate correlation between the tropopause height and the distance from the jet when the three stations (Dodge City, Kansas, Riverton, Wyoming, and Omaha, Nebraska) are south to the jet stream and north to the jet stream, respectively for 2003-4 winter. Again, the values followed by ± are one standard deviation.

(a)

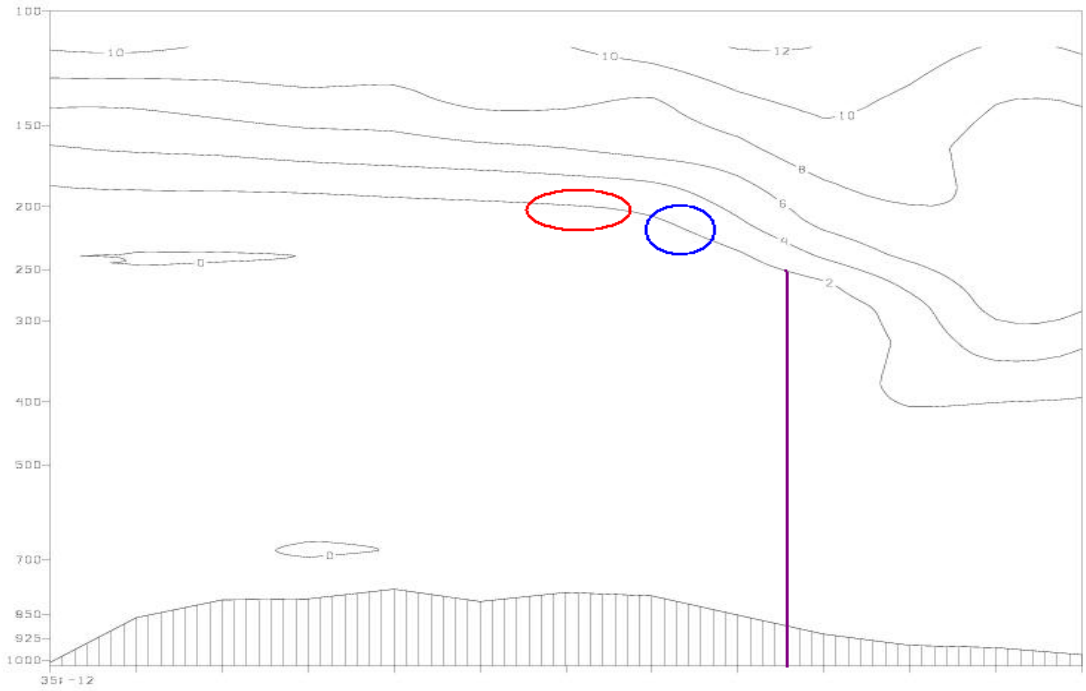
100
150
200
250
300
400
500
700
850
925
1000
35 -12

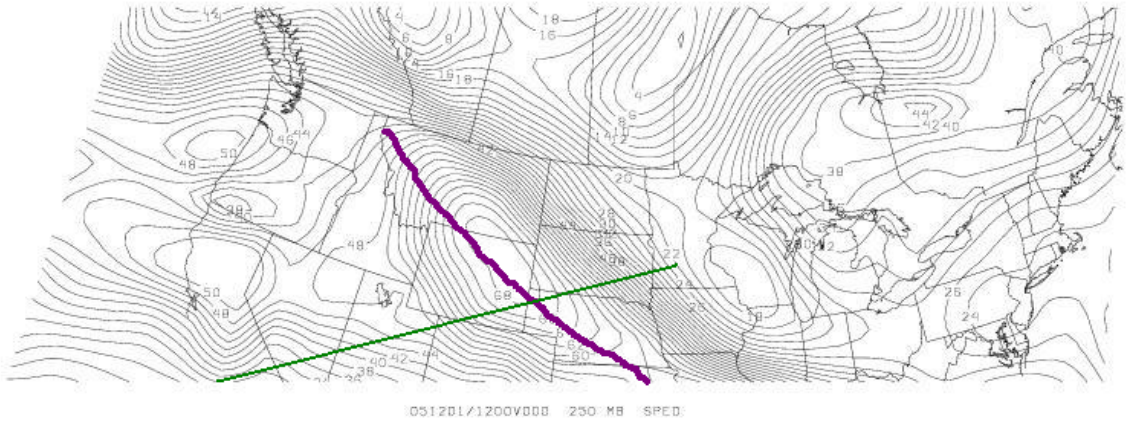
051201/1200V000 250 MB SPED

(b)

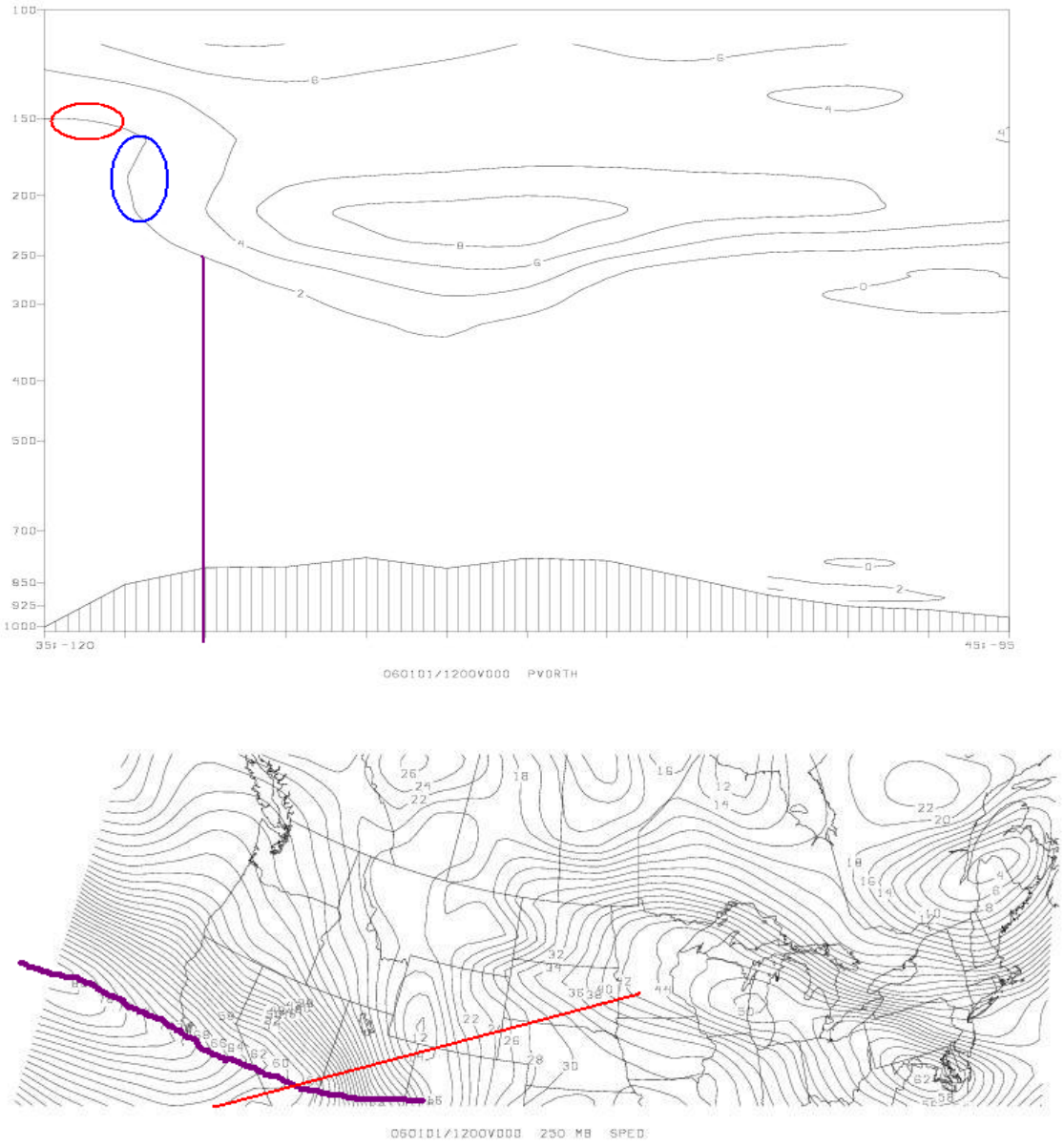

Figure 4.2 – The upper panels are potential vorticity contours and the lower panels are the isotachs at 250 MB at (a) 12Z, December 1st, 2005(b) 12Z, January 1st, 2006 for cross section from (35°N, 95°W) to (45°N, 120°W). The 2 PVU line can be taken as the tropopause. The purple lines indicate the location of the jet stream. The red lines in the lower panels are the cross-section from (35°N, 95°W) to (45°N, 120°W).

(a) Dodge City, Kansas

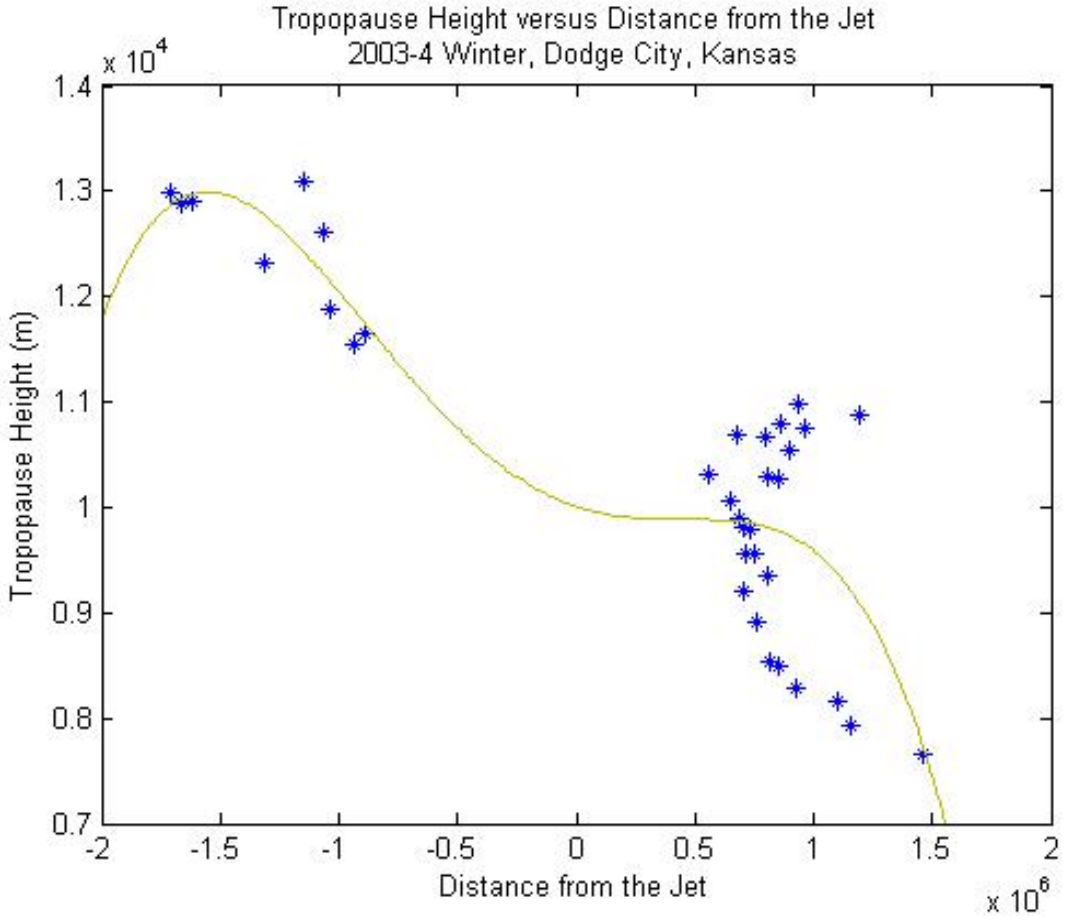

(b) Omaha, Nebraska

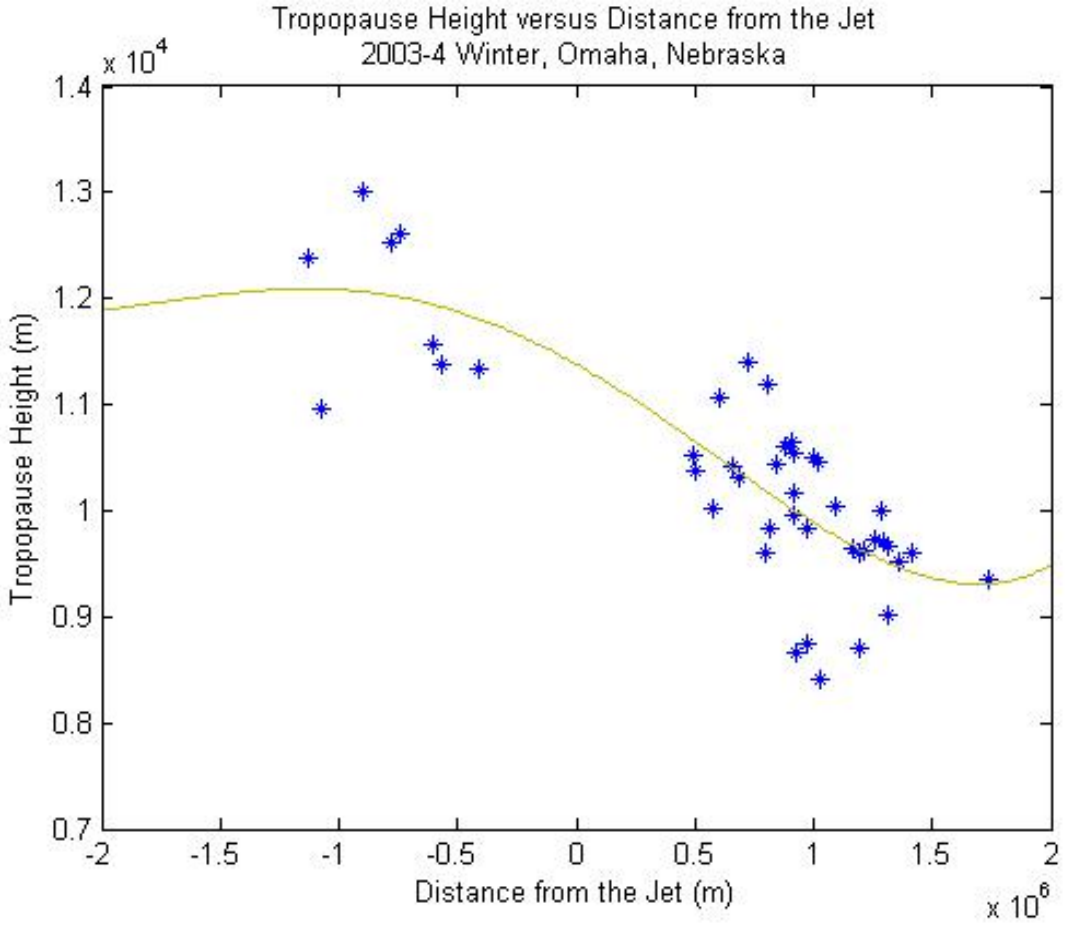

(c) Riverton, Wyoming

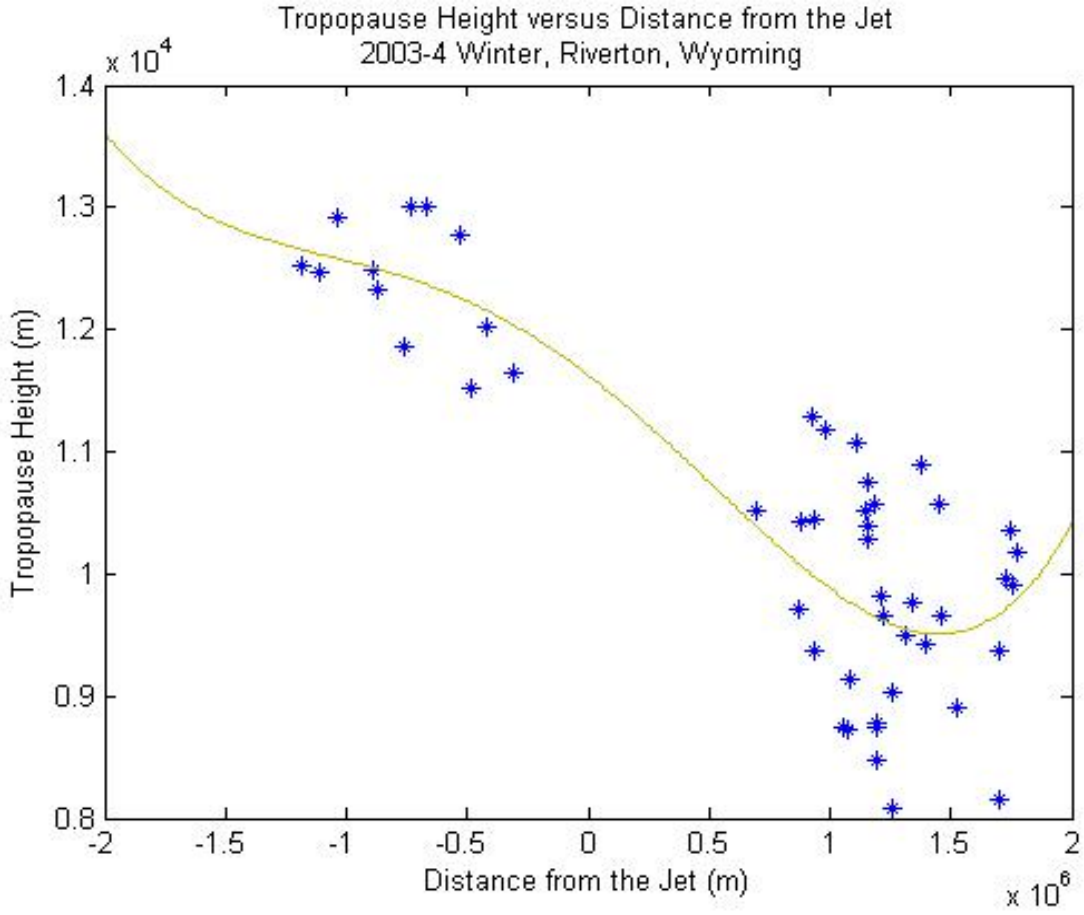

Figure 4.3 – The blue stars represent Tropopause Height versus Distance from the Jet for (a) Dodge City, Kansas (b) Omaha, Nebraska (c) Riverton, Wyoming. The green line is the 4th degree polynomial fitting curve. Negative (positive) distance denotes south (north) to the jet.

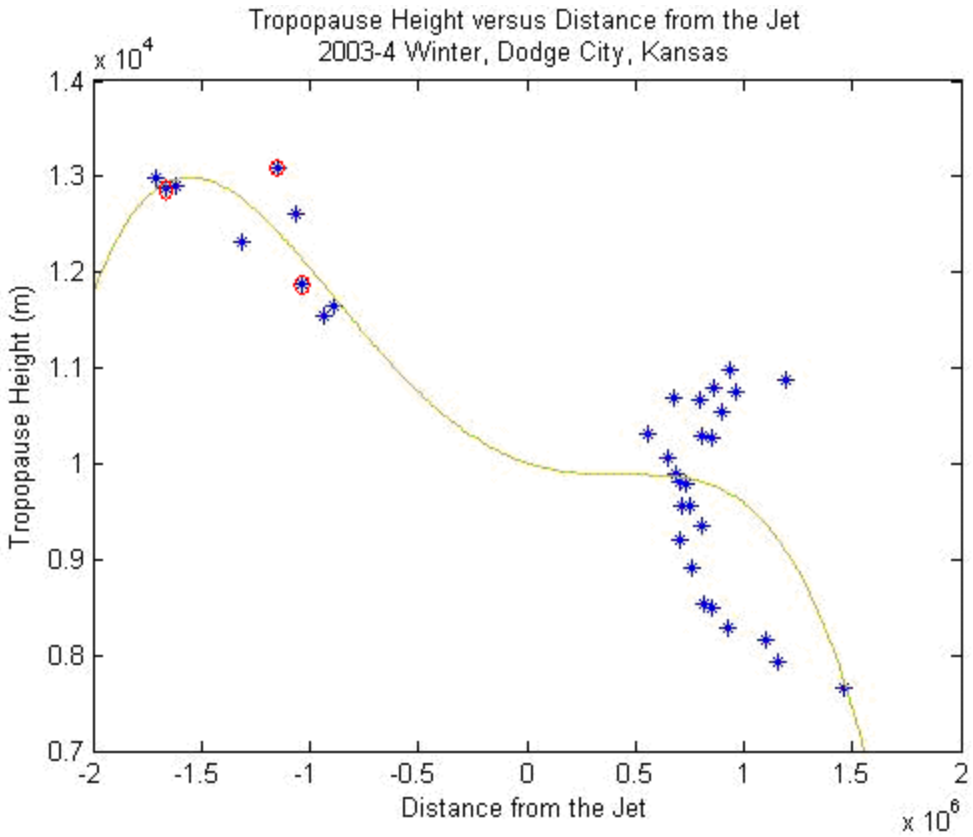

Figure 4.4 – The blue stars represent Tropopause Height versus Distance from the Jet for Dodge City, Kansas. The green line is the 4th degree polynomial fitting curve. Negative (positive) distance denotes south (north) to the jet. The 3 red circles denote the 3 cases corresponded to the cases in figure 4.5.

(a)

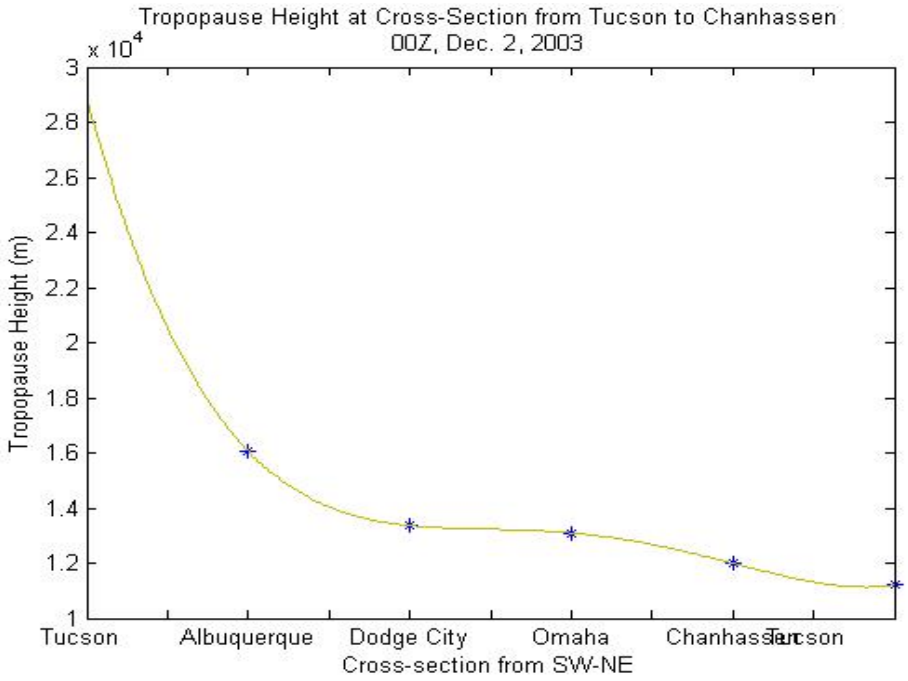
Tropopause Height at Cross-Section from Tucson to Chanhassen
00Z, Dec. 2, 2003
x 10^4
Tropopause Height (m)
3
2.8
2.6
2.4
2.2
2
1.8
1.6
1.4
1.2
1
Tucson
Albuquerque
Dodge City
Omaha
Chanhassen
Tucson
Cross-section from SW-NE

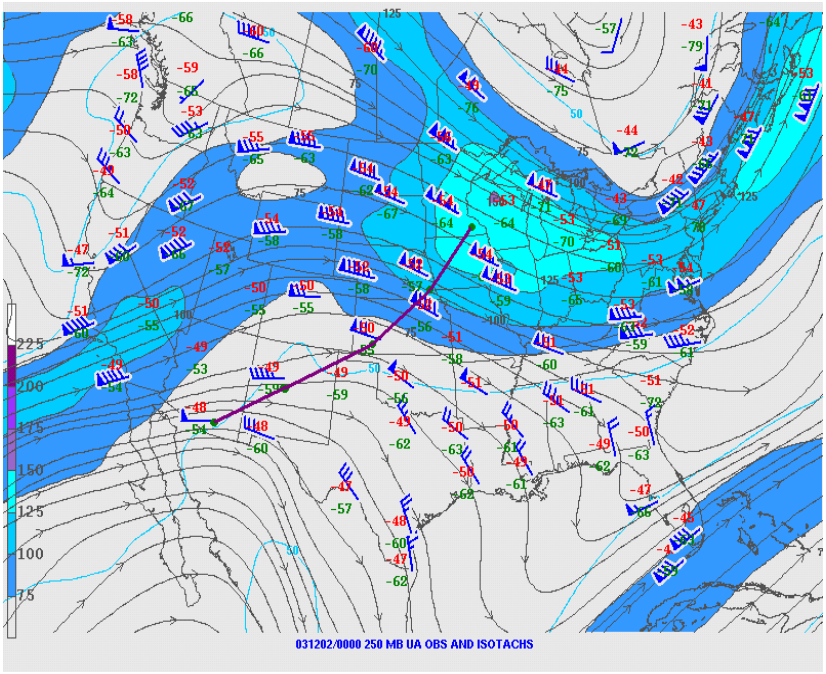
225
200
175
150
125
100
75
031202/0000 250 MB UA OBS AND ISOTACHS

(b)

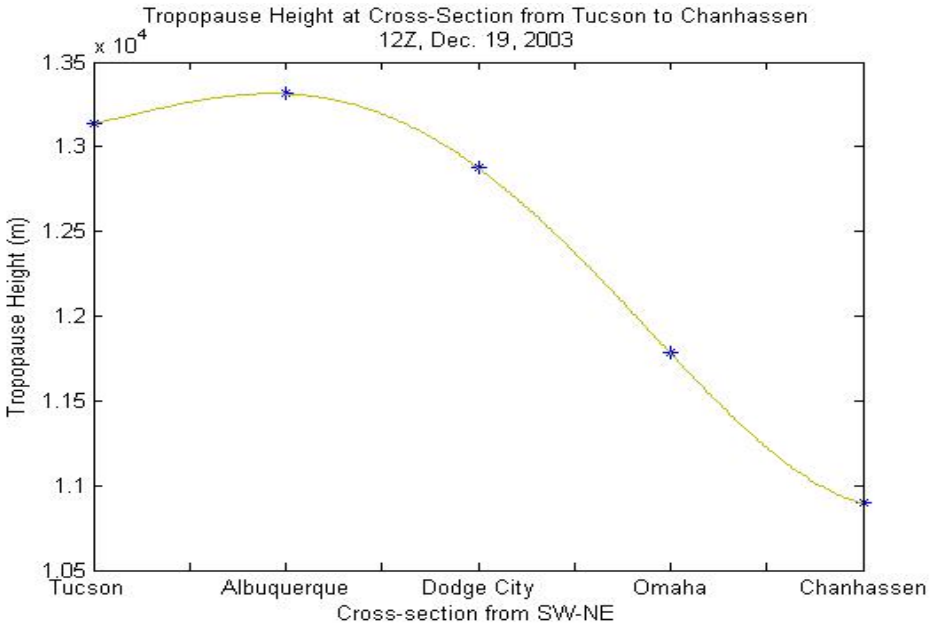
Tropopause Height at Cross-Section from Tucson to Chanhassen
12Z, Dec. 19, 2003
x 10^4
1.35
1.3
1.25
1.2
1.15
1.1
1.05
Tropopause Height (m)
Tucson
Albuquerque
Dodge City
Omaha
Chanhassen
Cross-section from SW-NE

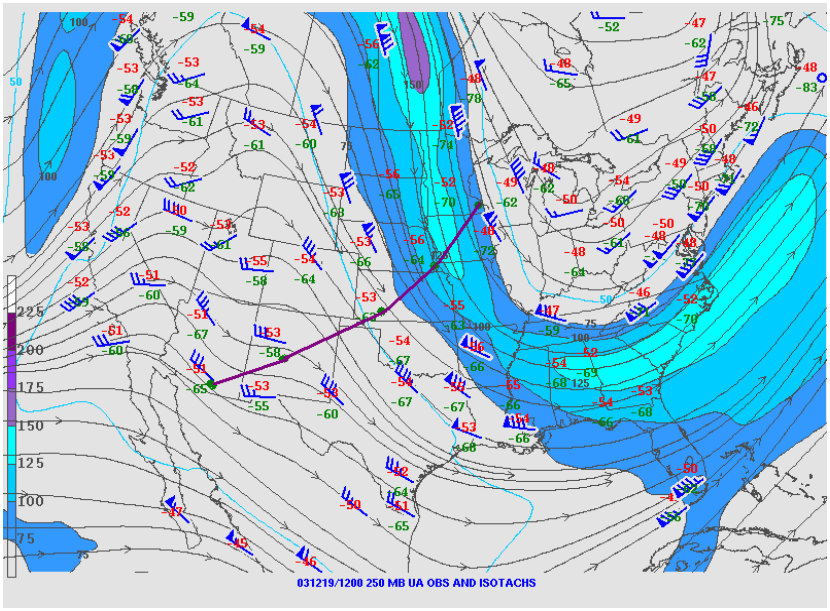
031219/1200 250 MB UA OBS AND ISOTACHS

(c)

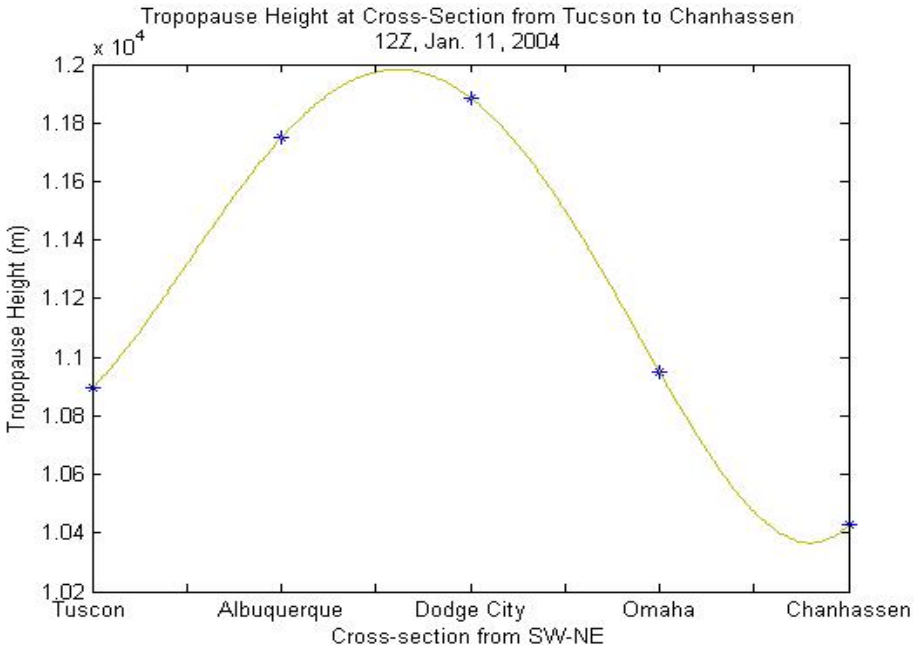

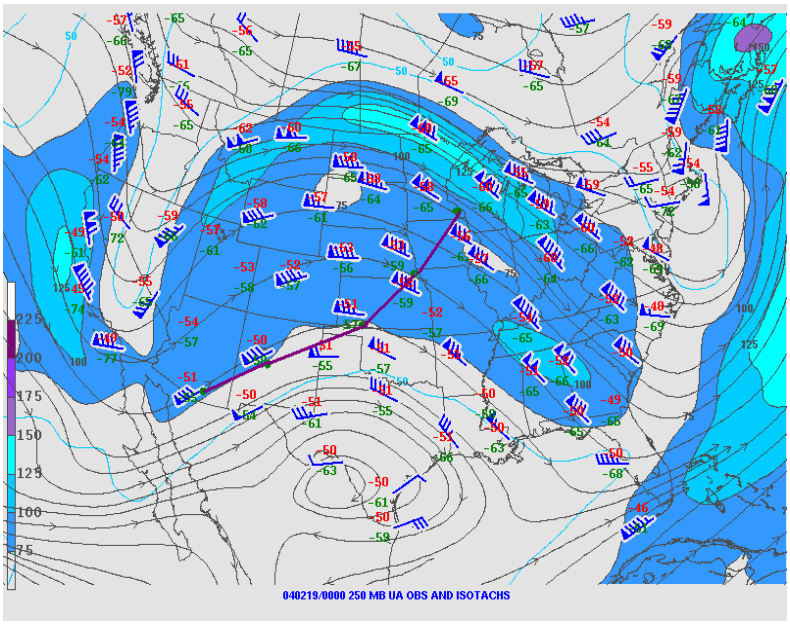

Figure 4.5 – The upper panels are the tropopause height at the cross-section of five stations (Tucson, Arizona, Albuquerque, New Mexico, Dodge City, Kansas, Omaha, Nebraska, and Chanhassen, Minnesota from Southwest to Northeast, respectively) from Tucson, Arizona to Chanhassen, Minnesota. The lower panels are 300 hPa height (black lines), and isotachs (contoured) which show the location of the jet streams at (a) 00Z, Dec. 2, 2003 (b) 12Z, Dec. 19, 2003 (c) 12Z, Jan. 11, 2004.

(a)

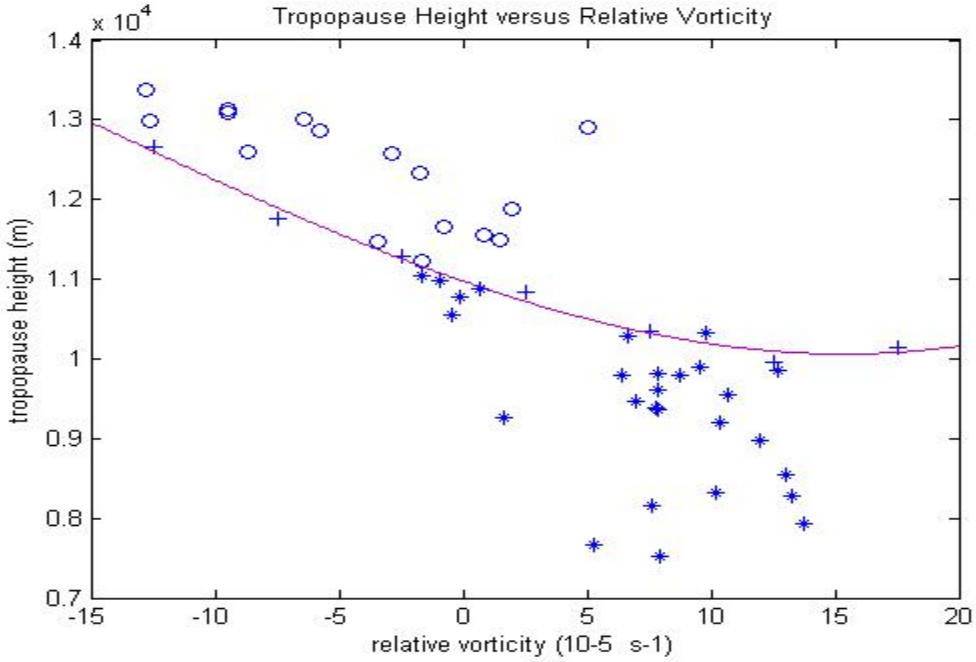
Tropopause Height versus Relative Vorticity
x 10^4
tropopause height (m)
relative vorticity (10-5 s-1)
1.4
1.3
1.2
1.1
1
0.9
0.8
0.7
-15
-10
-5
0
5
10
15
20

(b)

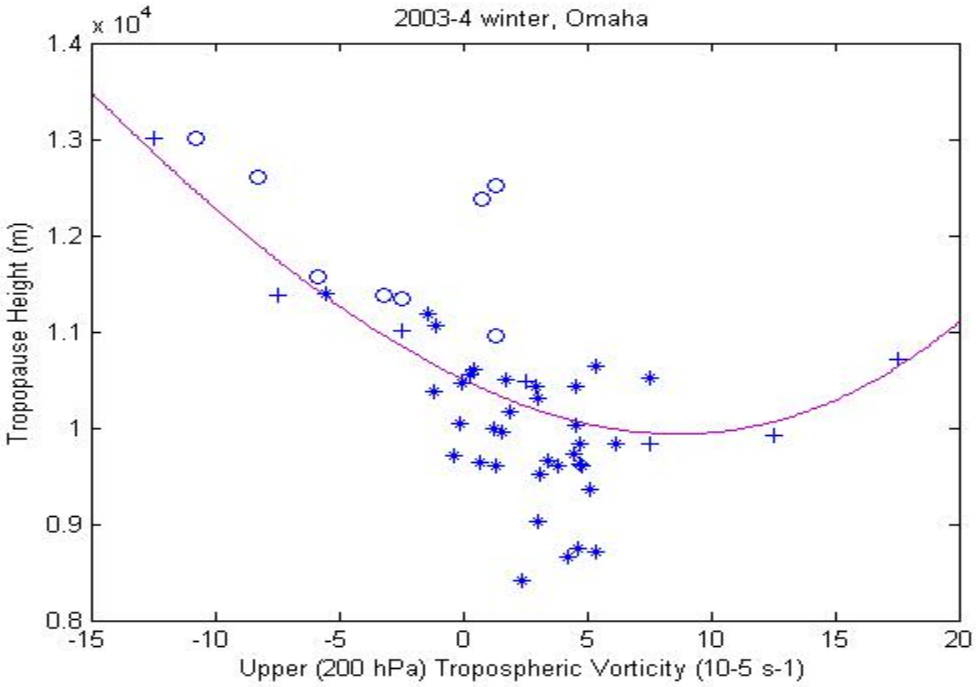
2003-4 winter, Omaha
x 10^4
Tropopause Height (m)
Upper (200 hPa) Tropospheric Vorticity (10-5 s-1)
1.4
1.3
1.2
1.1
1
0.9
0.8
-15
-10
-5
0
5
10
15
20

(c)

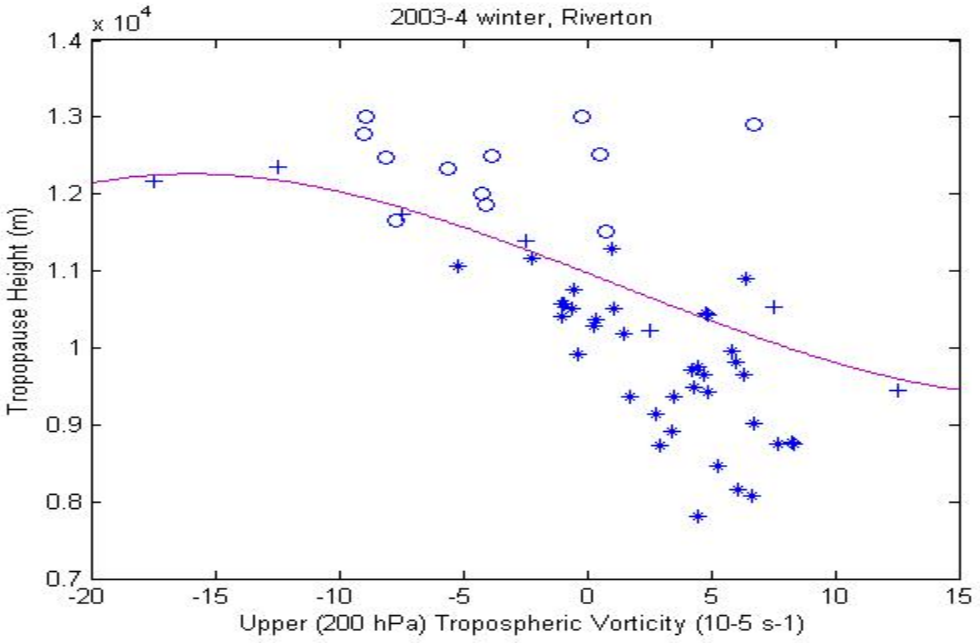

Figure 4.6 – Tropopause height (m) versus relative vorticity (10^{-5} s^{-1}) at 200 hPa for (a) Dodge City (b) Omaha (c) Riverton from December, 2003 to February, 2004. Plus signs are the average of tropopause height and the curve is the average tropopause height within each relative vorticity bin. Circles (Stars) are individual cases where the station is south (north) of the jet.

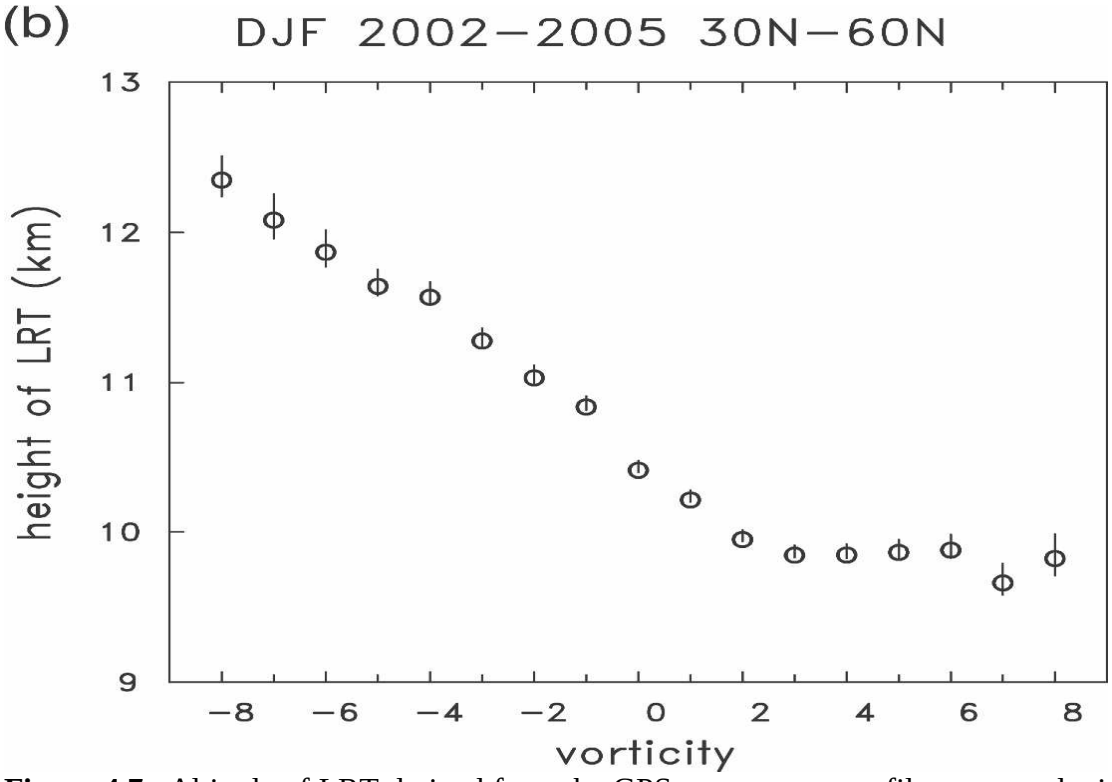

Figure 4.7 –Altitude of LRT derived from the GPS temperature profiles averaged within each vorticity (10^{-5} s^{-1}) bin. The circles show the mean values, and the error bars denote the std dev of the means (Figure (b) from Randel 2007).

	Dodge City (34 cases)	Omaha (43 cases)	Riverton (49 cases)
South of the Jet Stream	0.54±0.099	0.16±0.093	0.35±0.091
North of the Jet Stream	0.64±0.098	0.56±0.098	0.50±0.096

Table 4.7 – The separate correlation between the tropopause height and the upper relative tropospheric vorticity when the three stations (Dodge City, Kansas, Omaha, Nebraska and Riverton, Wyoming) are south to the jet stream and north to the jet stream, respectively for 2003-4 winter. The values followed by ± are one standard deviation.

5. Summary, Conclusions and Future Work

5.1 Summary

Building on previous research results of Birner et al. (2002), Birner (2006), Son and Polvani (2007), Wirth (2003) and others, additional understanding of processes that lead to the observed sharpness of the extratropical tropopause has been obtained. The main results of this thesis are as follows:

(1) I have reproduced, and somewhat extended, a pilot study from Bell's (2007) MS thesis and have shown that the extratropical tropopause is lifted in altitude and sharpened as a dry baroclinic wave passes over the station. These results are made clearer when the thermal tropopause is used as the geophysical reference level.

(2) Our hypothesis, that the distance from the jet is more important in determining the extratropical tropopause height than is the upper relative tropospheric vorticity is confirmed by comparing the partial correlations between the tropopause height and the upper relative tropospheric vorticity and that between the tropopause height and the distance from the jet for northern stations during a winter season.

5.2 Conclusions

In a previous effort, I tried to examine the relative contribution of dry dynamics and moist processes in leading to the observed extratropical tropopause structure (Juckes 2000). A dominant idea then was that balanced dynamics imply a sharper, higher extratropical tropopause when the upper tropospheric relative vorticity was anticyclonic, with the opposite being the case when the upper troposphere relative vorticity is cyclonic (Wirth 2002). An alternative concept follows from the seminal works of Held (1982) and Lindzen (1993), and that is that the sharpness of the extratropical tropopause is mainly a result of the sharpening of the vertical potential vorticity (PV) gradient by baroclinic mixing of the PV below the tropopause. A pilot study, largely reproduced from Bell's (2007) MS thesis showed that during the passage of a dry baroclinic wave, there was indeed lifting and sharpening of the extratropical tropopause.

An interesting result from Bell and Geller (2008) was that the curve showing the variation of the thickness of the extratropical stability transition layer (ESTL) with latitude shifted equatorward about 15° from summer to winter (see figure 5.1 from Bell and Geller, 2008). This is consistent with our hypothesis that the distance from the jet is important in determining the extratropical tropopause height since the Equator-to-Pole temperature difference in winter is larger and the jets then are shifted equatorward at this time. Figure 5.1 shows that the extratropical tropopause is less sharp in winter at given latitude (the tropopause is less sharp when the ESTL thickness is larger). Son and Polvani (2007) found that they could reproduce Bell and Geller's (2008) results by adjusting the specified pole-equator temperature difference in their simplified atmospheric general circulation model. Thus, our hypothesis that it is the distance from the jet that exerts the main control on the height of the extratropical tropopause and its thickness gives us a framework for understanding the cited Son and Polvani (2007) and Bell and Geller (2007) results.

Our study of 2 northern stations among the 3 in the extratropics shows that the distance from the jet is more important in determining extratropical tropopause height than the upper tropospheric relative vorticity. When we compare the correlations between

tropopause height and the station distance from the jet axis with the correlations between the upper tropospheric relative vorticity at the 2 northern stations, we find that the association with the distance from the jet is more important. This is not to say that Wirth's concept of balanced dynamics giving a higher and sharper tropopause when the upper troposphere relative vorticity is more anticyclonic is not valid. We do claim, however, that the distance from the jet axis exerts greater control over these tropopause variables especially at northern stations.

5.3 Suggestions for Future Work

Several studies have shown that the sharpness of the extratropical tropopause is mainly caused by the sharpening of the vertical potential vorticity (PV) gradient by baroclinic mixing of PV. It is also well known that a great deal of small-scale filamentary structure is seen at extratropical tropopause levels (Nielsen-Gammon, 2001). We believe that mixing of the large stratospheric PV values into the troposphere takes place by the baroclinic eddies shearing off high stratospheric PV filaments, which are then further sheared and mixed into the troposphere. By this process, the sharp PV boundary between the troposphere and stratosphere is lifted and sharpened further. This might explains why Son and Polvani's (2007) models gave sharper tropopause structures when the horizontal resolution was increased in a much more striking way than when the vertical resolution was increased. Both high vertical and horizontal resolution is likely needed to resolve the smaller PV filaments, and if these filamentary structures are not being resolved, the mixing process is not properly resolved, and numerically, this mixing looks like diffusion rather than filamentary mixing. It is interesting to note that while the high-reolution modeling of Miyazaki et al. (2010) gave a tropopause sharpness that compared reasonably with observations, they state the following. "Based on the comparison described here, however, the relative importance of horizontal and vertical resolutions on the TIL simulation is not clear."

This leaves us with two open questions. One is what horizontal and vertical resolutions are necessary to model realistically sharp extratropical tropopause structures. To answer this question, we wish to run very high resolution Held/Suarez-type GCMS in order to understand the vertical and horizontal resolution requirements to resolve the PV filaments, and thus the mixing process.

The other important question is what the importance of having a realistically sharp extratropical tropopause on troposphere-stratosphere exchange is. To answer this question, we will examine the stratosphere-troposphere mixing by looking at Lagrangian mixing of "clouds" of particles released in the lowermost stratosphere for different resolution models with differing tropopause sharpness in these Held-Suarez models.

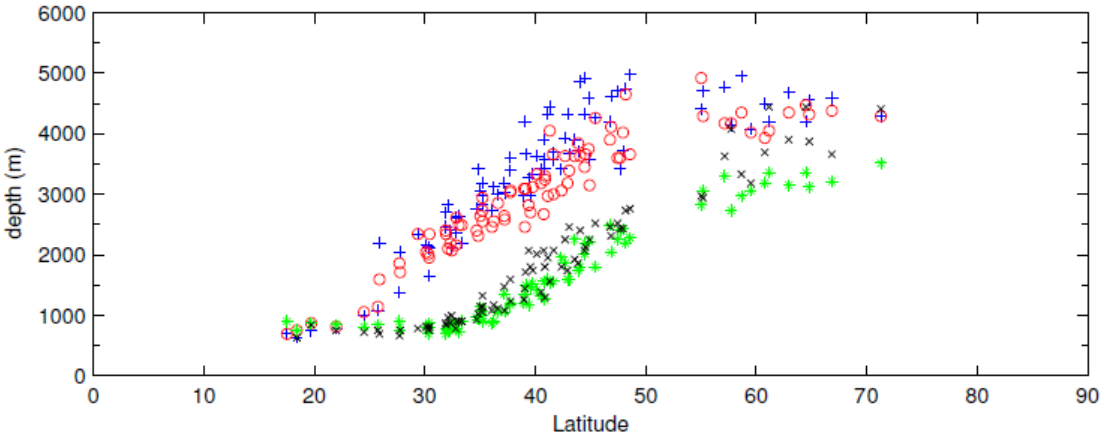

Figure 5.1 – Seasonally averaged latitudinal variability of the ESTL depth for high resolution data for DJF (blue +), MAM (red o), JJA (green *) and SON (black x). (Figure 4 from Bell (2008))

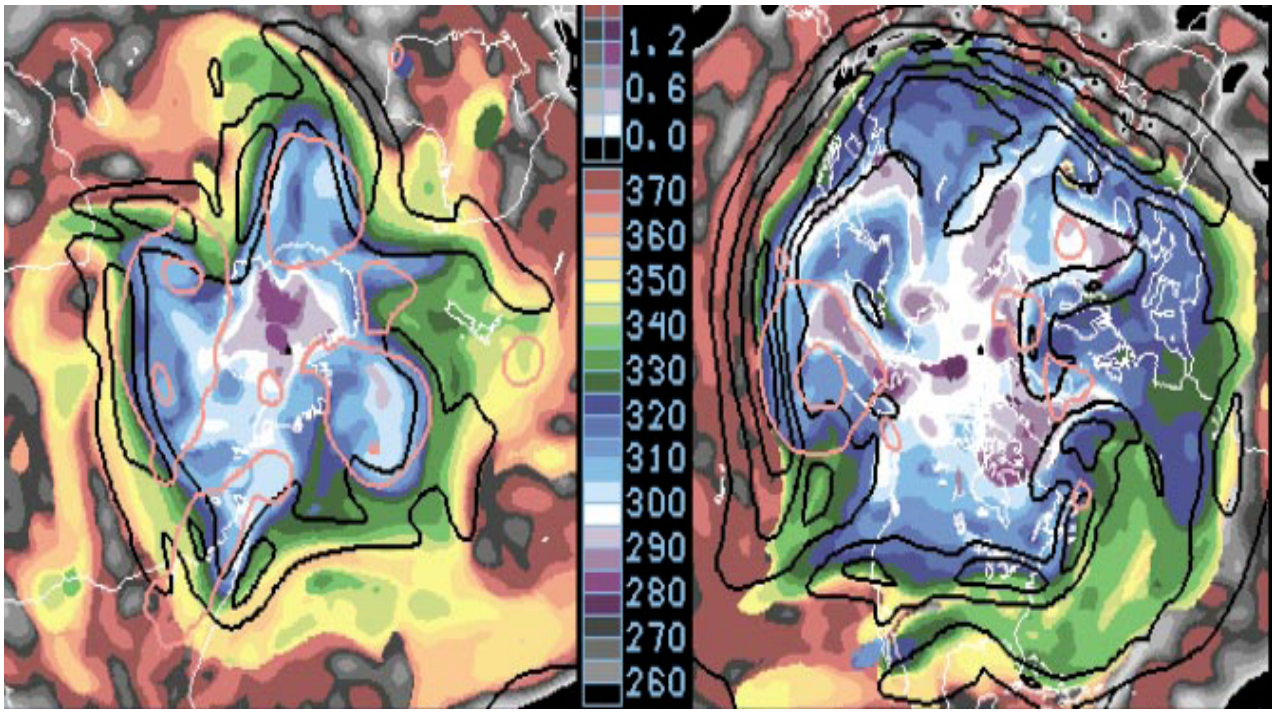

Figure 5.2 – Tropopause (1.5 PVU surface) potential temperature (in K) for 18Z on 2/1/97. Southern (Northern) Hemisphere is on the left (right). Black contours are 250-mb wind speed at 20 m/s increments starting at 30 m/s. (Figure 1 of Nielsen-Gammon (2001))

References:

Allen, S, and R. A. Vincent, 1995: Gravity wave activity in the lower atmosphere: Seasonal and latitudinal variations. *J. of Geophys. Res.*, 100, 1327-1350.

Barry, L., G. C. Craig, and J. Thuburn, 2000: A GCM investigation into the nature of baroclinic adjustment. *J. Atmos. Sci.*, 57, 1141-1155.

Bell, S. W. and M. A. Geller, 2008: Tropopause inversion layer: Seasonal and latitudinal variations and representation in standard radiosonde data and global models, *J. Geophys. Res.*, 113, D05109, doi:10.1029/2007JD009022.

Betts, A. K., 1986: A new convective adjustment scheme .1. Observational and theoretical basis. *Q. J. R. Meteorol. Soc.*, **112,** 677-691.

Birner, T., 2003: Die extratropische Tropopausenregion, *Res. Rep. DLR-FB-2004-17*, Dtsch. Zent. Fr Luft- und Raumfahrt, Cologne, Germany.

——, A. Dornbrack, and U. Schumann, 2002: How sharp is the tropopause at midlatitudes? *Geophys. Res. Lett.*, 29, 1700, doi:10.1029/2002GL015,142

——, 2006: Fine-scale structure of the extratropical tropopause region. *J. of Geophys. Res.*, 111, D04,104, doi:10.1029/2005JD006,301.

____, D. Sankey, and T. G. Shepherd, 2006: The tropopause inversion layer in models and analyses. *Geophys. Res. Lett.*, 33, L14804, doi:10.1029/2006GL026549.

Charney, J.G. 1947: The dynamics of long waves in a baroclinic westerly current. Journal of Meteorology 4, 135—62.

Eady, E. 1949. Long waves and cyclone waves. Tellus, 1, 33-52.

Geerts, B. and E. Linacre, 1997: Climate and weather explained. Routledge, London, H653.

Haynes, P., J. Scinocca, and M. Greenslade, 2001: Formation and maintenance of the extratropical tropopause by baroclinic eddies. *Geophys. Res. Lett.*, 28, 4179-4182.

Held, I. M., 1982: On the height of the tropopause and the static stability of the troposphere. *J. Atmos. Sci.*, 39, 412-417.

Highwood, E. J., and B. J. Hoskins, 1998: The tropical tropopause. Quart. J. Roy. Meteor. Soc., 124, 1579–1604.

Hoskins, B. J., M. E. Mclntyre, and A. W. Robertson (1985): On the use and significance of isentropic potential vorticity maps. Quart J. Roy. Meteor. Soc., 111, 877-946.

Hoskins, B. J. (1991): Towards a PV-Theta view of the general-circulation, Tellus, Ser. AB. 43, 27-35.

Hoerling, M. P., T. K. Schaack, and A. J. Lenzen, 1991: Global objective tropopause analysis. *Mon. Weather Rev.*, 119, 1816-1831.

Juckes, M. N., 2000: The static stability of the midlatitude troposphere: The relevance of moisture. *J. Atmos. Sci.*, 57, 3050-3057.

Lindzen, R. S., 1993: Baroclinic neutrality and the tropopause. *J. Atmos. Sci.*, 50, 1148-1151.

Manabe, S. and R. F. Strickler, 1964: Thermal equilibrium of the atmosphere with a convective adjustment. *J. Atmos. Sci.*, **21,** 361-385.

Miyazaki, K., S. Watanabe, Y. Kawatani, Y. Tomikawa, M. Takahashi, and K. Sato (2010), Transport and mixing in the extratropical tropopause region in a high□vertical□resolution GCM. Part I: Potential vorticity and heat budget analysis, J. Atmos. Sci., 67, 1293–1314.

Nielsen-Gammon, J. W., 2001: A visualization of the global dynamic tropopause. *Bull.Amer. Meteor. Soc.*, 82, 1151-1167.

Office of the Federal Coordinator for Meteorology (OFCM), 1997: Federal Meteorological Handbook No. 3: Rawinsonde and Pibal Observations. FCM-H3-1997, Washington, DC.

Randel, W.J., F. Wu and P. Forster, 2007: The extratropical tropopause inversion layer: Global observations with GPS data and a radiative forcing mechanism. *J. Atmos. Sci.*, 64, 4489-4496.

Schneider, T., 2004: The tropopause and the thermal stratification in the extratropics of a dry atmosphere. *J. Atmos. Sci.*, 61, 1317-1340.

Son, S.-W., and L. M. Polvani (2007): Dynamical formation of an extra-tropical tropopause inversion layer in a relatively simple general circulation model, Geophys. Res. Lett., 34, L17806, doi:10.1029/2007GL030564.

Stone, P. H., 1978: Baroclinic adjustment. *J. Atmos. Sci.*, 35, 561-571.

Stone, P. H. and J. H. Carlson, 1979: Atmospheric lapse rate regimes and their parameterization. *J. Atmos. Sci.*, 36, 415-423.

Thorncroft, C.D., B. J. Hoskins, and M. E. McIntyre (1993): Two paradigms of baroclinic-wave life-cycle behavior. Quart. J. Roy. Meteor. Soc., 119, 17-56.

Thuburn, J. and G. C. Craig, 1997: GCM tests of theories for the height of the tropopause. *J. Atmos. Sci.*, 54, 869-882.

Wirth, V., 2000: Thermal versus dynamical tropopause in upper-tropospheric balanced flow anomalies. *Q. J. R. Meteorol. Soc.*, 126, 299-317.

——, 2001: Cyclone-Anticyclone asymmetry concerning the height of the thermal and the dynamical tropopause. *J. Atmos. Sci.*, 58, 26-37.

——, 2003: Static stability in the extratropical tropopause region. *J. Atmos. Sci.*, 60, 1395-1409.

WMO, 1957: Meteorology-A three-dimensional science. *WMO Bulletin*, 6, 134-138.

Wilks, DS, 2005, Statistical Methods In The Atmospheric Sciences. Volume 100. Second edition.